Peptidyl-tRNA hydrolase is the nascent chain release factor in bacterial ribosome-associated quality control

Maxim S. Svetlov^{1,2#}, Clémence F. Dunand^{1,2}, Jose A. Nakamoto³, Gemma C. Atkinson³, Haaris A. Safdari⁴, Daniel N. Wilson⁴, Nora Vázquez-Laslop^{1,2}, Alexander S. Mankin^{1,2#}

- ¹ Center for Biomolecular Sciences, University of Illinois at Chicago, Chicago, IL 60607, USA
- ² Department of Pharmaceutical Sciences, University of Illinois at Chicago, Chicago, IL 60607, USA
 - ³ Department of Experimental Medicine, University of Lund, 221 00 Lund, Sweden
- ⁴ Institute for Biochemistry and Molecular Biology, University of Hamburg, 20146 Hamburg, Germany

Lead contact: Maxim S. Svetlov (msvet2@uic.edu)

Maxim S. Svetlov: msvet2@uic.edu; Alexander S. Mankin: shura@uic.edu.

[#] Corresponding authors:

SUMMARY

Rescuing of stalled ribosomes often involves their splitting into subunits. In many bacteria, the resultant large subunits bearing peptidyl-tRNAs are processed by the ribosome-associated quality control (RQC) apparatus that extends the C-termini of the incomplete nascent polypeptides with polyalanine tails to facilitate their degradation. While the tailing mechanism is well-established, it is unclear how the nascent polypeptides are cleaved off the tRNAs. We show that peptidyl-tRNA hydrolase (Pth), the known role of which has been to hydrolyze ribosome-free peptidyl-tRNA, acts in concert with RQC factors to release nascent polypeptides from large ribosomal subunits. Dislodging from the ribosomal catalytic center is required for peptidyl-tRNA hydrolysis by Pth. Nascent protein folding may prevent peptidyl-tRNA retraction and interfere with the peptide release. However, oligoalanine tailing makes the peptidyl-tRNA ester bond accessible for Pth-catalyzed hydrolysis. Therefore, the oligoalanine tail serves not only as a degron, but also as a facilitator of Pth-catalyzed peptidyl-tRNA hydrolysis.

INTRODUCTION

Cell growth and proliferation critically depends on efficient protein synthesis. While most mRNAs are smoothly translated by ribosomes, cleavage or chemical damage to mRNA, constellations of rare codons, or polymerization of problematic amino acid sequences can cause prolonged translational pausing (reviewed in ¹⁻³). Such ribosome stalling is detrimental to cells because it sequesters ribosomes together with the associated tRNAs in inactive states potentially leading to diminished global translation. In addition, the incomplete proteins trapped in the stalled ribosomes could be toxic for the cell. Therefore, organisms from all domains of life have evolved sophisticated mechanisms dedicated to rescuing and recycling stalled ribosomes and tRNAs and to targeting the associated truncated nascent peptides for degradation.

In eukaryotes, stalled ribosomes are recognized and split into subunits by the combined action of Hbs1/HBS1L, Dom34/Pelota(PELO) and Rli1/ABCE1 proteins (in yeast/mammals, respectively) ^{4,5}; reviewed in ⁶⁻⁸. While the resultant 40S subunits can readily reinitiate new rounds of translation, the split 60S subunits remain associated with peptidyl-tRNA (pept-tRNA). Such 60S-nascent chain complexes (60S-NCC) are targeted by the Ribosome-associated Quality Control (RQC) apparatus which recycles ribosomal subunits and tRNAs by facilitating the release of the nascent polypeptides while tagging them for degradation ⁹. These goals are achieved by the non-programmed addition of Ala- (in mammals) or Ala/Thr C-terminal tails ('CAT-tails', in yeast) to the nascent chains in a reaction catalyzed by the Rqc2/NEMF proteins ¹⁰. Tailing leads to extrusion of the nascent protein's lysine residues out of the nascent peptide exit tunnel of the ribosome allowing for their ubiquitination by the 60S-NCC associated Ltn1/Listerin ubiquitin E3 ligase ^{11,12}. The nascent chain ubiquitination promotes extraction and subsequent proteasomal degradation of the truncated proteins ^{11,13-15}. Additionally, in mammals, the Ala tails themselves serve as a degron recruiting other E3 ligases upon the release of the nascent protein ^{16,17}.

Recently, an RQC-like mechanism was discovered in bacteria ¹⁸. In *Bacillus subtilis* and a number of other bacterial species (**Figure 1A**), the RqcU (MutS2) protein senses ribosomes that have collided due to translational arrest and promotes splitting of the leading stalled ribosome into the small (30S) and large (50S) subunits ^{19,20}. The bacterial 50S-NCC is recognized by the NEMF ortholog RqcH which, in concert with RqcP, recruits Ala-tRNA^{Ala} to extend the C-terminus of the stalled polypeptide with an oligo-alanine tail ^{18,21,22}. Following release of the nascent chain from the ribosome, the oligo-Ala tail serves as a degron facilitating the hydrolysis of the incomplete

protein by the ClpXP protease ¹⁸. The 50S-NCC can also accumulate in bacteria that lack the RqcU/RqcH/RqcP system due to translation of specific ribosome-destabilizing nascent peptide sequences ^{23,24}, antibiotic treatment ²⁵, heat shock ^{26,27} and possibly other stresses ^{28,29}.

A critical step in recycling of 60S- or 50S-NCC is the eventual uncoupling of the nascent peptide (Ala/CAT-tailed or not) from the associated tRNA. Only after disengaging from tRNA, the nascent chain can be extracted from the exit tunnel, the tRNA released, and the large subunit made available for new rounds of translation. In eukaryotes, the 60S-NCC associated pept-tRNA, carrying a ubiquitinated nascent chain, is targeted by Vms1/ANKZF1 nuclease. This enzyme disengages the protein from tRNA by endonucleolytically cleaving off the tRNA's CCA end 30-33 rather than by hydrolyzing the pept-tRNA ester bond, as it occurs during conventional translation termination promoted by release factors. In contrast, in bacteria, it has remained unknown which cellular factor is responsible for the release of the nascent peptide from the 50S-NCC and how the release is coordinated with the RQC-catalyzed Ala-tailing. Several bacterial proteins have been proposed to carry out this task, including the canonical (RF1, RF2) and non-canonical (ArfB, PrfH) release factors, some yet to be discovered endonuclease analogous to the eukaryotic Vms1/ANKZF1, or peptidyl-tRNA hydrolase (Pth), an enzyme known to hydrolyze ribosome-free pept-tRNAs ^{1,21,26,27,34}. However, in the absence of experimental evidence, none of these proteins so far stand out as strong candidates. Indeed, association of release factors with the ribosome is driven to a large extent by their contacts with the small ribosomal subunit and they are unlikely to bind to the isolated large ribosomal subunit; bacterial endonucleases with the activity akin to that of Vms1/ANKZF1 are unknown; the remaining candidate, Pth was described as an enzyme acting upon pept-tRNAs that drop off the ribosome primarily at the early rounds of translation ^{35,36}. Furthermore, if Pth were to act upon the 50S-NCC, how would it access the ester bond of the pepttRNA enclosed within the active site of the peptidyl transferase center (PTC) of the large subunit?

In this paper, we reveal that stalled pept-tRNA in bacterial 50S-NCC is in fact released by the action of Pth. We show that pept-tRNA needs to be partially extracted (pulled back) from the 50S-NCC to render it accessible for Pth-catalyzed hydrolysis. We further show that Ala-tailing facilitates the exposure of the pept-tRNA ester bond when the folding of the nascent protein prevents its extraction from the 50S-NCC. Our findings establish Pth as an integral component of RQC irrespective of whether it acts in concert with the Ala-tailing system or as a part of alternative ribosome rescue mechanism(s).

RESULTS

Pth is genetically linked to the RQC pathway.

Genes with related functions tend to be closely clustered in bacterial genomes ³⁷. Therefore, we reasoned that the gene encoding the factor responsible for hydrolyzing pept-tRNA in 50S-NCC may be located in the neighborhood of the genes encoding the Ala-tailing machinery. Examining the *B. subtilis* genome, we found the Pth-encoding gene *pth* in close vicinity of *rqcP* that encodes the RqcP protein, the key accessory factor that facilitates RqcH-catalyzed addition of the oligo-Ala tails (**Figure 1B**). In two other *rqcH*-positive bacterial species, *Streptococcus pneumoniae* and *Staphylococcus aureus*, *pth* and *rqcP* even reside in the same operon (**Figure 1B**). These initial observations prompted us to systematically analyze the proximity of *pth* and *rqcP* across fully-sequenced reference bacterial genomes. The results of this analysis (**Figure 1C**) showed strong genomic association of the *pth* and *rqcP* genes specifically in *rqcH*-positive bacteria (**Figure 1C** and **Table S1**), suggesting that *pth* may be functionally related to the RQC pathway.

We then asked whether Pth is genetically linked to the RQC mechanism. Because Pth is essential for bacterial growth and its gene cannot be deleted, we utilized the *B. subtilis pth* knockdown (pth-KD) strain in which pth expression is downregulated through inhibition of its promoter by catalytically-dead dCas9 paired with sgRNA pth 38. As expected, even though pth-KD cells showed diminished growth they could nevertheless readily form colonies on agar plates. Both, the pth-KD and $\Delta rqcH$, strains could also grow on plates with subinhibitory concentrations of tetracycline (**Figure 1D**), an antibiotic that causes genome-wide collisions of translating ribosomes and accumulation of substrates for the RQC pathway 18,39 . However, $\Delta rqcH$ cells where Pth expression was repressed became hypersusceptible to this antibiotic (**Figure 1D**). Synthetic hypersensitivity to tetracycline showed that not only Pth is genomically associated with one of the key RQC components (**Figure 1C**), but it is also potentially functionally involved in the RQC pathway (**Figure 1D**), possibly playing a role in the release of nascent peptides from 50S-NCC.

Pth can release Ala-tailed nascent peptides from the 50S-NCC

To explore a potential mechanistic role of Pth in the RQC pathway, we established an in vitro assay for monitoring the disengagement of an Ala-tailed nascent polypeptide from tRNA in a 50S-NCC (Figure 2A). The assay exploits the observation that newly translated firefly luciferase (Luc) remains inactive until it is released from the tRNA and its C-terminus is fully extracted from the ribosomal nascent peptide exit tunnel ^{40,41}. To prepare 50S-NCC, a non-stop mRNA encoding Luc followed by a seven alanine residues-long tail (Luc-Ala₇) was translated in vitro by B. subtilis or Escherichia coli ribosomes. Following translation, ribosomes stalled at the 3' end of the mRNA were dissociated into subunits and 50S-NCC were isolated by sucrose gradient centrifugation (**Figure S1A**). We then treated the *B. subtilis* 50S-Luc-Ala₇-tRNA complexes with lysates of *B*. subtilis pth-KD cells with normal or reduced level of Pth expression and followed protein release in real time by appearance of luminescence. Luc-Ala₇ release was notably slower in lysates prepared from cells with diminished Pth expression compared to those with normal Pth activity (Figure 2B). However, comparable levels of luminescence were reached in either of the lysates when 50S-NCC were treated with puromycin, an antibiotic which facilitates nascent chain release by serving as a peptide acceptor in the PTC (reviewed in 42). The results of these experiments implicate Pth in hydrolyzing oligo-Ala tailed peptidyl-tRNA trapped on 50S-NCC, thereby, supporting the notion that Pth may participate in the RQC pathway.

RQC-mediated Ala-tailing of the nascent peptide facilitates its release from the 50S subunit.

Because in RqcH-positive bacteria a significant fraction of nascent chains in the 50S-NCC undergo Ala-tailing, we asked whether the ability of Pth to release Luc from 50S-NCC depends upon the presence of the Ala-tail at the C-terminus of the nascent peptide. To address this question, we compared the kinetics of release of untailed or Ala₇-tailed Luc. Remarkably, the absence of the Ala₇-tail markedly decreased the rate of Luc release from *B. subtilis* 50S-NCC (**Figure 3A**), revealing the stimulatory role of the C-terminal oligo-Ala sequence in pept-tRNA hydrolysis. Consistently, even though an Ala-tailing machinery has not been described for *E. coli*, the Pth-catalyzed release of Luc from *E. coli* 50S-NCC was stimulated by the presence of the Ala₇ C-terminal tail (**Figure S2A**). The release of untailed Luc was even less efficient in lysates prepared

from *B. subtilis pth*-KD or *E. coli* with reduced Pth activity (**Figure S3**), confirming that Pth is responsible for the nascent chain decoupling from tRNA.

We wondered if release of untailed Luc from the 50S-NCC was stimulated by the RqcH/RqcP-mediated Ala tailing. We found, that in comparison with wt *B. subtilis* lysate, the release of Luc from 50S-NCC was significantly less efficient in lysates prepared from $\Delta rqcH$ or $\Delta rqcP$ strains (**Figure 3B**) which, while being deficient in Ala-tailing, possessed wild-type levels of Pth activity. Restoring the Ala-tailing potential by mixing the lysates from $\Delta rqcH$ or $\Delta rqcP$ strains accelerated the release of the untailed Luc to levels comparable to those observed in wt cells lysate (**Figure 3B**). Not surprisingly, release of the 'pre-tailed' nascent protein from 50S:Luc-Ala₇-tRNA complexes was affected to a lesser extent by the absence of RqcH or RqcP in the cell lysates (**Figure 3B**).

The antibiotic thiostrepton has been reported to inhibit Ala-tailing by impeding the interaction of RqcH with 50S subunits ^{22,43}. Consistent with the stimulatory role of Ala-tailing for the Pth-mediated pept-tRNA hydrolysis in the 50S-NCC, addition of thiostrepton to cell lysates inhibited the release of untailed Luc from 50S-NCC but did not importantly impact the release of the Ala-tailed protein (**Figure 3C**). Antibiotics that inhibit elongation factors EF-Tu (kirromycin) or EF-G (fusidic acid), which are also thiostrepton targets but are not involved in Ala-tailing, had no effect on the release of untailed or tailed-nascent proteins (**Figure 3C**).

The presented data suggest that after ribosome splitting, 50S-NCC-associated Luc-tRNA remains largely inaccessible to Pth until Ala-tailing of the nascent protein catalyzed by the RQC machinery sensitizes pept-tRNA to Pth action. To directly test this hypothesis, we reconstituted in vitro the tailing/release system from purified *B. subtilis* proteins, i.e., each one of the individual components of the Ala-tailing apparatus (tRNA^{Ala}, alanyl-tRNA synthetase, and the RQC factors RqcH and RqcP) and Pth (**Figure 3D**). While Pth alone, without Ala-tailing machinery, was unable to release untailed Luc from 50S-NCC, efficient release was observed in the presence of RQC factors and Ala-tRNA. Stimulation of the Pth-mediated Luc release was likely due to the Alatailing reaction, rather than to the mere association of RqcH and RqcP with 50S-NCC, since withdrawal of any single RQC component, including Ala-tRNA^{Ala}, from the tailing/release system, resulted in background levels of pept-tRNA hydrolysis (**Figure 3D**). Combined, our data highlight

the importance of the Ala-tailing machinery for Pth-mediated release of the nascent protein from *B. subtilis* 50S-NCC.

Having established the importance of the nascent chain Ala-tailing for the Pth-catalyzed pept-tRNA hydrolysis in 50S-NCC, we next determined the length requirement of the C-terminal oligo-Ala sequence for efficient peptide release. Untailed Luc-tRNA in the 50S-NCC was largely impervious to hydrolysis by purified Pth (**Figure 4A**). Addition of a single alanine residue to the C-terminus of Luc only slightly improved the Pth-mediated pept-tRNA hydrolysis, whereas the presence of Ala₃-, Ala₅- or Ala₇-tails greatly stimulated the release of the nascent protein (**Figure 4B**). Because the stimulatory effect of the Ala tail plateaued at 5-7 Ala residues, most of the rest of the experiments were carried out with the Ala₇ tail. Importantly, Luc-tRNA and Luc-Ala₇-tRNA non associated with ribosomes could be hydrolyzed by Pth with equally high efficiencies (**Figure S4C**), indicating that untailed Luc-tRNA is a poor Pth substrate only when within the large ribosomal subunit and that Ala-tailing facilitates Pth-mediated hydrolysis specifically in the 50S-NCC.

Consistent with the conservation of the ribosome structure and properties across bacterial species, the presence of the Ala tail stimulated the Pth-catalyzed release of Luc also from *E. coli* 50S-NCC (**Figure S4**). Because of the similarity of the effects, we carried out some of the subsequent experiments using *E. coli* 50S-NCC which can be more readily generated in the cell-free translation system.

The nature of the C-terminal tail is important for nascent peptide release from the 50S-NCC

We wondered whether it is the mere presence of extra C-terminal amino acids or if also the tail's amino acid identity is important for stimulating the release of the nascent chain from the 50S-NCC. Strikingly, changing the Ala-tail of Luc-Ala₇ to the other possible hepta homopeptides reduced the efficiency of the Pth-mediated release. Thus, while in the 50S-NCC context, Luc-Ser₇ was hydrolyzed nearly as efficiently as Luc-Ala₇, release of Luc nascent chains appended with Tyr-, Trp-, Leu-, Pro-, Arg- or Lys- tails was very inefficient and comparable to that of the untailed protein (**Figure 4C**). tRNAs esterified with Luc carrying Phe₇, Ile₇, Met₇, His₇, Gln₇, Glu₇, Asn₇, Gly₇, Asp₇, Val₇, or Thr₇ tails were hydrolyzed by Pth with intermediate efficiencies. Luc-Cys₇

lacked enzymatic activity which prevented testing the efficiency of its release from 50S-NCC. Importantly, among all the tested heptapeptide tails, Ala₇ was the most efficient in promoting pept-tRNA hydrolysis and thus, 50S subunit recycling.

These results allowed us to conclude that the amino acid identity of the C-terminal tail introduced by the RQC system is important not only for the subsequent degradation of the truncated protein, but also for the release of the nascent peptide from the 50S-NCC.

Retraction of the pept-tRNA and exposure of its ester bond is required for its Pth-catalyzed hydrolysis in 50S-NCC

We asked why Ala-tailing facilitates pept-tRNA hydrolysis specifically in the context of 50S-NCC. *In silico* structural analysis shows that the ester bond of the pept-tRNA residing in the ribosomal PTC is sterically inaccessible to Pth (**Figure 5A-C**). Thus, for productive hydrolysis by Pth, the pept-tRNA ester bond needs to disengage from the PTC active site while retracting its nascent chain 'backwards' through the exit tunnel. Ala-tailing may directly or indirectly facilitate the "retrosliding" of the nascent chain.

To test whether nascent chain retrosliding is a prerequisite for Pth-catalyzed pept-tRNA hydrolysis in 50S-NCC, we exploited the Zn²⁺-dependent folding of the Zn-finger ADR1a domain. A previous study has shown that folding of ADR1a in the vestibule near the opening of the ribosomal exit tunnel exerts a pulling force on the peptide segment tethering ADR1a to tRNA ⁴⁴, and thus should prevent nascent protein retrosliding and pept-tRNA retraction (**Figure 5D**). We prepared 50S-NCC, in which the tRNA moiety and the ADR1a domain of the pept-tRNA were separated by a 29 amino acid long linker – a length sufficient for Zn²-mediated ADR1a folding in the vestibule section of the exit tunnel near its opening on the solvent side of the 50S subunit ⁴⁴. We then analyzed the efficiency of pept-tRNA hydrolysis by Pth in the presence of ZnCl₂ or of Zn²⁺ chelator TPEN. When ZnCl₂ was present and ADR1a could fold into a compact structure, pept-tRNA was resistant to the Pth-catalyzed hydrolysis. In contrast, it was readily hydrolyzed under Zn²⁺-depletion conditions when ADR1a was unfolded, and the nascent chain could likely retroslide through the exit tunnel (**Figures 5E and S6A**). Importantly, the presence of ZnCl₂ had little effect upon the ability of Pth to release Luc-Ala₇ (whose folding is Zn²⁺ independent) from the 50S-NCC (**Figure S5B**), or to hydrolyze ribosome-free peptidyl-tRNA (**Figure S5C**).

Increasing the length of the linker separating tRNA from ADR1a facilitated pept-tRNA hydrolysis (**Figure 5F-H**), likely because additional slack in the nascent peptide segment between the tRNA and ADR1a domain allows retraction of the pept-tRNA from the PTC. Consistently, with a more abridged linker (16 amino acid-long), which is too short to allow for the ADR1a domain to fold in the vestibule, the dependence of pept-tRNA hydrolysis by Pth in the presence of Zn²⁺ became less pronounced (**Figure 5F-H**). These data are consistent with the model that retraction of the pept-tRNA from the PTC is required for its hydrolysis by Pth and that protein folding within or outside of the exit tunnel can sterically block retrosliding of the nascent chain, thereby preventing pept-tRNA release from the 50S-NCC and interfering with recycling of the large ribosomal subunit.

We then reasoned that Ala-tailing may promote hydrolysis of the pept-tRNA in the Pthresistant 50S-NCC by introducing extra slack in the nascent peptide and facilitating retrosliding that is otherwise blocked by protein folding. Indeed, addition of Ala-tails of increasing length to the C-terminus of the ADR1a-containing constructs facilitated Pth-catalyzed hydrolysis of the pept-tRNA in 50S-NCC, even when the folding of the nascent chain would prevent its retrosliding through the exit tunnel (**Figures 51,J and S6D**). Finally, consistent with the idea that hydrolysis of the 50S subunit-associated pept-tRNA is promoted by tailing, preincubation of the Pth-resistant 50S-NCC in our in vitro reconstituted tailing/release system facilitated Pth-mediated peptide release when all the components of the Ala-tailing machinery were present (**Figure 5K**).

Thus, Ala-tailing of a non-retractable nascent protein in the 50S-NCC facilitates its release by making possible the interaction of the Pth active site with the pept-tRNA ester bond. The results obtained with the ADR1a-based reporter likely explain the sluggish release of untailed Luc from the 50S-NCC (**Figures 3A and S2A**), which is likely prevented by the folding of the nascent Luc protein outside the ribosome near the tunnel exit.

Antibiotics that stabilize pept-tRNA in the PTC and prevent its retraction interfere with the Pth-catalyzed release of the nascent chain from the 50S-NCC

Several antibiotics that interact with the large ribosomal subunit make direct contacts with either the P-site tRNA (sparsomycin, blasticidin S) ^{45,46} or the nascent chain that protrudes from the PTC into the exit tunnel (linezolid, chloramphenicol) ^{47,48}. Preincubation of the 50S-NCC carrying Luc-Ala₇-tRNA with such antibiotics significantly inhibited pept-tRNA hydrolysis

(**Figure S2B**). In contrast, antibiotics that target the initiation complex (retapamulin) (**Figure S2B**) or the elongation factors (kirromycin, fusidic acid) (**Figure 3C**) had no effect. Thus, small molecules that impede the disengagement of the pept-tRNA from the PTC or interfere with retrosliding of the nascent peptide in the tunnel prevent Pth-catalyzed hydrolysis of the 50S-NCC-associated pept-tRNA.

DISCUSSION

We have presented evidence here that the release of pept-tRNA from the 50S-NCC is catalyzed by Pth revealing this enzyme as a critical component of the RQC pathway. We show that to become susceptible to Pth-catalyzed hydrolysis, the pept-tRNA needs to be dislodged from the PTC of the 50S-NCC and retracted so that its ester bond becomes accessible to the Pth active site.

Based on the presented data, we propose a model for the role of Pth in the mechanism of the ribosome and tRNA recycling as well as its interplay with the Ala-tailing machinery in RqcHpositive bacteria such as B. subtilis (Figure 6). When translation arrest results in ribosome collision, RqcU promotes ribosome splitting 19. Conceivably, ribosome splitting could also be collision- and RqcU-independent and caused by other factors. Irrespective of the cause, dissociation of the translating ribosome into subunits results in formation of the 50S-NCC (stage 1). If the nascent polypeptide is free to retroslide through the exit tunnel, pept-tRNA can easily detach from the PTC. In the absence of the small ribosomal subunit, pept-tRNA is retained in the 50S-NCC primarily due to the threading of the nascent peptide through the exit tunnel, whereas direct interactions of the tRNA with the PTC are limited to weak contacts of its CCA end with the 23S rRNA ^{49,50}. Therefore, with the freely sliding nascent chain, thermal movement of pept-tRNA in the 50S-NCC would likely be sufficient to expose its ester bond to Pth (stage 2), leading to pept-tRNA hydrolysis (stage 3). However, retrosliding of the nascent protein would likely be often prevented by its folding, specific contacts with the tunnel walls, anchoring within the translocon, cotranslational interactions with chaperones, or by jamming the tunnel with small molecule ligands such as antibiotics or metabolites (reviewed in ⁵¹). In this case, the ester bond of the pept-tRNA cannot be properly exposed, binding of Pth to the 50S-NCC becomes futile and, instead, recruitment of the Ala-tailing machinery prevails (stage 4). Addition of Ala residues to the C-

terminus of the nascent chain (**stage 5**) may facilitate retrosliding by either displacing the tightly folded protein domains or the nascent chain cellular interacting partners away from the exit tunnel, or by breaking interactions of the stuck polypeptide with the tunnel walls. In the process of Alatailing, RqcP stabilizes pept-tRNA in the PTC, preventing a productive contact of Pth with the 50S-NCC. Depending on the processivity of Ala-tailing and the kinetics of binding/dissociation of RqcH/RqcP or Pth, none of which are currently known, Pth may probe the 50S-NCC at each cycle of Ala incorporation or after addition of several Ala residues (**stage 6**). In any case, once the Alatail reaches a length sufficient for the proper exposure of the pept-tRNA ester bond by retrosliding-mediated retraction, Pth manages to hydrolyze the pept-tRNA and the nascent protein can be finally released (**stage 7**). Accordingly, we propose that in the RQC pathway, Ala-tailing of stuck peptides serves two functions: 1) promoting rapid degradation of the truncated proteins by appending an oligo-Ala degron, as demonstrated previously ¹⁸, and 2) facilitating the Pth-promoted release of the nascent polypeptide from 50S-NCC, expediting recycling of the tRNA and the large ribosomal subunit.

We found that in comparison to all other amino acid homo-oligomers, C-terminal tails composed of Ala residues are particularly beneficial for pept-tRNA hydrolysis in the 50S-NCC. Tailing with some other small (Ser, Thr, Val, Gly) or negatively charged (Asp, Glu) amino acids also stimulates release of non-retractable nascent chains. In contrast, positively charged (Arg, Lys), or bulky (Phe, Trp, Tyr) amino acids, as well as Pro residues do not stimulate 50S-NCC recycling. Why are Ala-tails specifically favorable for pept-tRNA hydrolysis in the 50S-NCC? It has been shown that free, N-acetyl-Ala-tRNA^{Ala} is particularly efficiently hydrolyzed by Pth in comparison with other N-acetyl-aminoacyl-tRNAs 52. Thus, tailing specifically with Ala may be favorable for Pth activity upon 50S-NCC. However, because the rates of hydrolysis of other model pept-tRNA substrates with varying amino acids 52 do not correlate closely with their ability to stimulate the release of the stuck peptide from the 50S-NCC, we favor the hypothesis that, regardless of their efficiency as Pth substrates, Ala-tails facilitate the nascent peptide retrosliding better than other Cterminal oligomers. Interactions of the nascent chain with the PTC-proximal segment of the exit tunnel are particularly important for translation ^{36,53-55}. Noteworthy, amino acid residues composing the 'release non-stimulating' tails are known to establish strong interactions with the PTC-proximal segment of the exit tunnel ^{24,56,57}, possibly preventing nascent chain retrosliding. The 'non-sticky' nature of the oligo-Ala tail may be particularly favorable for mobilizing the

nascent protein stuck in the ribosomal exit tunnel. Hence, along with its ability to signal protein degradation, the evolutionary selection of Ala-tailing as a preferred C-terminal modification for faulty nascent peptides was likely driven by the ability of the tail to facilitate pept-tRNA retraction and being an adequate Pth substrate.

Pth was originally characterized as a protein in charge of hydrolyzing free pept-tRNAs that prematurely dissociate from translating ribosomes ^{35,36,58}. Regeneration of the cellular pool of deacylated tRNAs necessary for translation is believed to underly the essentiality of Pth in bacteria ^{59,60}. Our present work and observations of others ²³ have shown that the cellular functions of Pth extend beyond the hydrolysis of free-floating pept-tRNAs revealing the role of this essential enzyme in the ribosome rescue pathway where it facilitates recycling of not only tRNAs, but also of the large ribosomal subunits. The contribution of Pth functions in ribosome rescue to its essentiality in bacterial cells awaits investigation.

While in RqcH-positive bacteria Ala-tailing targets truncated proteins for degradation by appending a C-terminal degron, Ala- or CAT-tailing in eukaryotes serves a similar goal primarily by helping the ubiquitination of the nascent chains ^{11,12}. Non-programmed addition of C-terminal residues by the RQC machinery forces extrusion of lysine residues of the nascent protein chain buried in the exit tunnel allowing their ubiquitylation by the 60S-NCC-associated Ltn1/Listerin ubiquitin ligase ^{11,12}. Conceivably, ubiquitination of the nascent chain may sterically prevent its retrosliding through the tunnel. Hence, maybe not surprisingly, release of ubiquitinated nascent chains from 60S-NCC is catalyzed not by hydrolysis of the pept-tRNA ester bond, but by the cleavage of the tRNA's CCA end by Vms1/ANKZF1, an endonucleolytic activity which does not require pept-tRNA retraction from the PTC ³⁰⁻³³. Remarkably, in vitro data suggest that the release of the non-ubiquitinated pept-tRNA from the 60S-NCC can be promoted by Pth1, the eukaryotic ortholog of the bacterial Pth. Similar to Pth in bacteria, Pth1 action likely requires pept-tRNA retrosliding that would be abolished by the nascent chain ubiquitination ³³.

In *B. subtilis* and likely in other bacteria that exploit the RqcH/RqcP-dependent Ala-tailing of the nascent peptide in 50S-NCC, Pth operates as a component of the RQC pathway. However, many bacteria that lack RqcH and, thus, presumably incapable of nascent peptide tailing, still possess the RqcP ortholog Hsp15, which interacts specifically with 50S-NCC ^{26,27,61}. The omnipresence of RqcP homologs suggests that 50S-NCC accumulation is common even in bacterial species lacking the Ala-tailing machinery. Splitting of the translating ribosome into

subunits can result from heat shock and other stresses ^{26,27,61}, action of specific ribosome-splitting factors ^{25,29,62-65}, and likely other effectors. Our data show that, like Pth in *B. subtilis*, *E. coli* Pth can also release the nascent protein from 50S-NCC. These results are consistent with the previous reports showing that Pth is involved in releasing polypeptides from *E. coli* 50S-NCC generated during translation of the so-called intrinsic ribosome destabilization sequences ^{23,24}. Extrapolating our finding, it is reasonable to expect that hydrolysis of the 50S-NCC-associated pept-tRNA in RqcH-negative bacteria also relies on retrosliding of the nascent peptide in the exit tunnel and dislodging of pept-tRNA from the PTC. Some cellular polypeptides, for example, intrinsically unfolded proteins, can be particularly prone to retrosliding. Retrosliding of others, however, may be cumbersome. In our experiments, retrosliding could be prevented by assembly of the compact ADR1a domain inside the exit tunnel and, likely, by folding of the nascent Luc protein outside the ribosome. In the absence of the C-terminal tailing mechanism, other yet unidentified factors might facilitate the exposure of the pept-tRNA ester bond to the Pth action on 50S-NCC.

Our findings may help to develop antibacterial therapies targeting bacteria-specific ribosome rescue pathways ^{66,67}. Given the difference in strategies for pept-tRNA release from 50S-and 60S-NCC in bacteria and eukaryotes, respectively, and the lack of structural conservation of bacterial and eukaryotic peptidyl-tRNA hydrolases, bacterial Pth emerges as an attractive antibiotic target. Due to the essentiality of Pth in bacteria, inhibiting its activity should arrest cell growth and proliferation by preventing recycling of drop-off pept-tRNAs or hydrolysis of the pept-tRNA in the 50S-NCC. Furthermore, our data show that antibiotics that prevent pept-tRNA retraction by either interfering with the retrosliding of the protein chain through the exit tunnel or by locking pept-tRNA in the PTC interfere with the Pth-catalyzed release of the pept-tRNA from 50S-NCC. Hence, these antibiotics emerge as not only direct blockers of protein synthesis but also as inhibitors of ribosome rescue. Consistently, diminishing Pth activity sensitizes bacteria to the action of several ribosome-targeting inhibitors ⁶⁸⁻⁷⁰. Therefore, successful Pth inhibitors are expected to act synergistically with some of these drugs, potentiating their action against pathogenic microorganisms.

LIMITATIONS OF THE STUDY

While the extent of the pulling force upon the nascent protein chain afforded by the ADR1a domain folding in the tunnel's vestibule has been investigated ^{44,71}, the details of Luc folding outside the ribosome are unknown. Similarly, it remains to be investigated how the sequence of the nascent protein spanning the exit tunnel affects its retrosliding ability.

Finally, the details of the interplay of Pth and RqcH/RqcP with the 50S-NCC rely on the kinetics of binding and dissociation of these proteins to the 50S subunit with the tRNA molecule exposed at the interface side of the subunit. Additional ensemble or single-molecule experiments will be needed to deduce these kinetics parameters which will help to refine the proposed model.

ACKNOWLEDGEMENTS

We thank Vasili Hauryliuk and Tatsuaki Kurata (Lund University) for providing the Δ*rqcH B. subtilis* strain and plasmids encoding *B. subtilis* RqcH and RqcP, Gunnar von Heijne (Stockholm University) for the plasmids with the ADR1a constructs, Egor Syroegin and Alena Aleksandrova (University of Illinois at Chicago) for providing ErmDL-tRNA, tRNA^{Ala} and Ala-RS and Yury Polikanov (University of Illinois at Chicago) for help with the analysis of structural data and helpful discussions. This work was supported by the grant from the National Science Foundation MCB-1951405 (to N.V.-L. and A.S.M.), the Knut and Alice Wallenberg Foundation (2020.0037 to G.C.A.), and the Swedish Research council (2019-01085 and 2022-01603 to GCA).

AUTHOR CONTRIBUTION

Conceptualization, M.S.S., A.S.M., and N.V.-L.; Methodology, M.S.S., A.S.M., G.C.A.; Investigation, M.S.S., C.F.D., J.A.N., and H.A.S; Writing – Original Draft, M.S.S., N.V.-L.; Writing – Final Manuscript, Review & Editing, A.S.M., N.V.-L., and M.S.S.; Funding Acquisition: N.V.-L., A.S.M., G.C.A., D.N.W.; Resources, N.V.-L., A.S.M., G.C.A., D.N.W.; Supervision, M.S.S., G.C.A., and D.N.W.

DECLARATION OF INTERESTS

The authors declare no competing interests.

MAIN FIGURE TITLES AND LEGENDS

Figure 1. Pth is genetically and functionally linked to the bacterial RQC pathway

- (A) Bacterial ribosome-associated quality control (RQC) pathway ^{8,19}. The factor responsible for disengaging the tRNA and the nascent peptide in the 50S-NCC remains unknown.
- (B) Location of the *pth* gene in the neighborhood of *rqcP* (*yabO*) in the genomes of *rqcH*-positive bacterial species *B. subtilis*, *Streptococcus pneumoniae* and *Staphylococcus aureus*. Location of the putative transcription termination sites ⁷²⁻⁷⁴ is indicated by black loops.
- (C) Left: Distance (number of genes) separating *pth* and *rqcP* genes in the genomes of 767 RqcH-positive bacteria (light red bars) or separating *pth* and the rqcP ortholog *hslR* (*hsp15*) in 2616 RqcH-negative bacteria (blue bars). Bin size is 100 genes. Right: zoomed in section of the 0-50 genes distance of the histogram of RqcH-positive bacteria shown on the left. Bin size is 2 genes. See also Table S1.
- (D) Spot test showing sensitivity to tetracycline of *B. subtilis* $\Delta rqcH$ cells with decreased expression of Pth. Both, WT and Pth-KD cells express dCas9; Pth-KD strain also expresses *pth*-specific sgRNA ³⁸.

Figure 2. Pth in *B. subtilis* lysates hydrolyzes Ala-tailed peptidyl-tRNAs on split 50S subunits

- (A) Principle of the luciferase-based nascent peptide release assay. Luciferase gains activity only after its release from the ribosome ⁴⁰.
- (B) Release of Luc-A₇ polypeptide from 50S-NCC in lysates of Pth-KD *B. subtilis* cells. Decreased expression of Pth in Pth-KD cells is induced by the addition of xylose. Puromycin addition (arrow) releases residual luciferase from the 50S-NCC. The bar graph shows the efficiency of Pth-mediated release in lysates from cells with normal- (uninduced, gray trace) or low- (xylose-induced, orange trace) Pth expression, estimated relative to the luciferase activity achieved after puromycin treatment. The error bars show the SD in four independent experiments. See also Figure S1A.

Figure 3. RQC-mediated oligoalanine tailing facilitates Pth-mediated hydrolysis of pept-tRNA in the 50S-NCC

- (A) Release of untailed (Luc) and tailed (Luc-Ala₇) luciferase from 50S-NCC in *B. subtilis* lysates. Following incubation with lysates, complexes were treated with puromycin. Luminescence achieved after puromycin treatment was set as 100%. Bar graph shows Pthmediated luciferase release relative to that following puromycin treatment. See also Figures S2A and S3A.
- (B) Efficiency of release of untailed or Ala₇-tailed luciferase in lysates of wild-type, $\Delta rqcH$ or $\Delta rqcP$ *B. subtilis* cells. 'Lysate mix' sample had a 1:1 mixture of lysates of $\Delta rqcH$ and $\Delta rqcP$ cells.

- (C) Effects of antibiotics that interfere with Ala-tailing (thiostrepton, Ths) or not (fusidic acid, Fus, or kirromycin, Kir) on Pth-promoted release of untailed (gray bars) or Ala₇-tailed (red bars) luciferase from 50S-NCC in wt *B. subtilis* lysate. See also Figure S2B.
- (D) Release of untailed luciferase from 50S-NCC in an in vitro-reconstituted Alatailing/release system composed of its purified protein components (RqcH, RqcP, Ala-RS, Pth) and tRNA^{Ala}. Release efficiency was estimated relative to that afforded by puromycin treatment. The Coomassie- or ethidium bromide- stained gels of the purified components are shown on the left.
- (A-C) Error bars show SD from four (A-B) or three (C-D) independent experiments.

Figure 4. Properties of the C-terminal tail impact the efficiency of Pth-mediated release of nascent proteins from 50S-NCC

- (A) Release of untailed (Luc) and tailed (Luc-A₇) luciferase from *B. subtilis* 50S-NCC by purified *B. subtilis* Pth, and then by puromycin treatment. See also Figure S4.
- (B and C) Release efficiencies of nascent luciferase in (B) *B. subtilis* 50S-NCC, C-terminally extended with the indicated number of alanine residues or (C) nascent luciferase, in *E. coli* 50S-NCC, extended with different heptapeptide C-terminal tails. In (B) and (C), release carried out by purified respective Pth was estimated as a ratio of luminescence produced by Pth treatment relative to that that following puromycin treatment. Error bars show SD from three independent experiments.

Figure 5. Nascent protein folding can interfere with Pth-catalyzed pept-tRNA hydrolysis in 50S-NCC

- (A) Model of a 50S-NCC representing 50S subunit associated with pept-tRNA (from the cryo-EM structure of a stalled translation complex, PDB: 3J9W ⁷⁵).
- (B) Modeled structure of the Pth-tRNA complex (from the x-ray structure of the Pth complexed with the tRNA analog, PDB: 3VJR ⁷⁶).
- (C) Superposition of the structures shown in A and B by aligning the tRNA bodies. Shown in red are Pth residues that would sterically clash with elements of the 50S subunit.
- (D) Schematics of the experimental setup. With a 29-amino acid long linker, Zn²⁺-mediated folding of ADR1a in the vestibule of the ribosomal exit tunnel ⁴⁴ should prevent nascent peptide retrosliding and pept-tRNA retraction.
- (E, J, K) Hydrolysis of the pept-tRNA in *B. subtilis* 50S-NCC by purified *B. subtilis* Pth. Reactions were performed in the absence (TPEN) or presence of Zn²⁺, as indicated. [³⁵S]-labeled unreactive peptidyl-tRNA or Pth-hydrolyzed peptide product were gel-separated and detected by autoradiography. Experiments shown in panels E and J were also carried out with *E. coli* 50S-NCC (see Figure S5A and D).
- (E) Peptide release from the complex shown in (D).
- (F) Constructs like in (D) but with linkers of varying length.

- (G) Peptide release from the complexes shown in (F) carried out using *E. coli* 50S-NCC and purified *E. coli* Pth.
- (H) Relative efficiency of peptidyl-tRNA hydrolysis as function of the length of the linker estimated from the gels shown in (G). Error bars represent SD from three independent experiments.
- (I) The construct like in (D) but C-terminally extended with the number of alanine residues indicated in (J).
- (J) Peptide release from the 50S-NCC carrying peptidyl-tRNAs derived from the constructs shown in (I).
- (K) Release of the peptide derived from the construct shown in (D) in the presence of the indicated purified components of the Ala-tailing/release system.

Figure 6. Role of Pth in tailing-independent and tailing-dependent ribosome rescue pathways:

Tailing independent:1, ribosome splitting; 2, pept-tRNA retraction; 3, Pth-catalyzed pept-tRNA hydrolysis.

Tailing-dependent: 1, ribosome splitting; 4, tailing machinery recruitment; 5, Ala-tailing, 6,7, Pth-catalyzed pept-tRNA hydrolysis attempted either at (6) each round of Ala-addition or (7) after synthesis of the Ala tail of specific length.

STAR Methods

Key resources table

REAGENT or RESOURCE	SOURCE	IDENTIFIER
Antibodies	COUNCE	IDENTIFIER
Artibodies		
Bacterial and virus strains		
	DOCO	4 4 4
B. subtilis 168	BGSC	1A1
B. subtilis dCas9	BGSC	1A1278
B. subtilis dCas9/sgRNA ^{pth}	BGSC	BEC00530
B. subtilis ΔrqcH::spcR	Crowe-McAuliffe et al.	VHB256
B. subtilis dCas9/sgRNA ^{pth} ΔrqcH::spcR	This paper	
E. coli C600	Cruz-Vera et al. 77	N/A
E. coli C600 pth(Ts)	Cruz-Vera et al. 77	N/A
E. coli SQ171 pAM55-2	Orelle et al. 78	N/A
E. coli JM109	Promega	PR-L2001
E. coli BL21(DE3)	Sigma	CMC-0016
Biological samples		
Chemicals, peptides, and recombinant proteins		T =
Spectinomycin	Fisher Scientific	Cat#215899305
Chloramphenicol	Fisher Scientific	BP904-100
Erythromycin	Sigma-Aldrich	E6376
Ampicillin	Sigma-Aldrich	A9518
Xylose	Fisher Scientific	AC141001000
RNase-free DNase I	Roche	Cat#04716728001
Lysozyme	Sigma-Aldrich	L4919-1G
EasyTag™ EXPRESS35S Protein Labeling Mix, [35S]-	Perkin Elmer	NEG772002MC
D-Luciferin	Fisher Scientific	Cat#88293
Puromycin	Sigma-Aldrich	P7255
TPEN	Sigma-Aldrich	P4413
ErmDL-tRNA	Syroegin et al. 48	N/A
Complete Protease Inhibitor cocktail	Sigma-Aldrich	Cat#11836153001
zampiano i retodo i milato oconon	9	
Critical commercial assays		
PURExpress Δ (aa, tRNAs) Kit	NEB	E6840S
PURExpress Δ Ribosome Kit	NEB	E3313S
Custom PURExpress Δ (aa, tRNAs) Δ Ribosome Kit	NEB	N/A
Phusion High-Fidelity DNA polymerase	NEB	M0530S
Gibson Assembly Master Mix	NEB	E2611S
Deposited data	This paper	https://data.mendele y.com/datasets/kng9 rzcx3d/1
Oligonucleotides		

See Table S2	This paper	N/A
Recombinant DNA		
pCA24N-pth(Ec)	Kitagawa et al. ⁷⁹	N/A
pCA24N-pth(Bs)	This paper	N/A
pET24d-rqcH-HTF	Takada et al. 43	N/A
pET24d-rqcP-TEV-His ₆	Takada et al. 43	N/A
pLAS	Nilsson et al. 44	N/A
pBESTluc™	Promega	L492A-C
Software and algorithms		
MAFFT L-INS-i version 7.453	Katoh et al. 80	https://mafft.cbrc.jp/a lignment/software/
HMMER v3.3.2	HMMER	hmmer.org
TrimAl v1.2	Capella-Gutierrez et al. 81	http://trimal.cgenomi cs.org/downloads
IQ-TREE v1.6.12	Nguyen et al. 82	http://www.iqtree.cibiv.univie.ac.at/
JalView v.2.11.2.0	Waterhouse et al. 83	https://www.jalview.o rg/download/
FigTree v.1.4.4	Andrew Rambaut Group	https://github.com/ra mbaut/figtree/
FlaGs	Saha et al. 84	https://github.com/G CA-VH-lab/FlaGs2
UCSF Chimera	Pettersen et al. 85	https://www.cgl.ucsf. edu/chimera/downlo ad.html
Prism 9	GraphPad	https://www.graphpa d.com/
ImageJ	Schneider et al. 86	https://imagej.net/ij/i ndex.html
R version 4.2.2	The R Project for Statistical Computing	https://cran.r- project.org/mirrors.ht ml
Other		
Zirconium Beads	BioSpec	Cat#11079101Z
HisTrap HP column	GE Healthcare	Cat#17-5248-01
HiTrap Butyl FF column	GE Healthcare	Cat#17-5197-01
Microplate reader Infinite M200Pro	Tecan	Cat#30050303
Prep homogenizer	MP Biomedicals	Cat#116004500

Lead contact

Further information and requests for resources and reagents should be directed to and will be fulfilled by the lead contact, Maxim Svetlov (msvet2@uic.edu).

Materials availability

This study did not generate new unique reagents.

Data and code availability

This paper analyzed publicly available genomic data from the National Center for Biotechnology Information using software described in the papers cited in the References section.

This paper does not report original code.

The original data for the gels and agar plates are deposited to Mendeley (https://data.mendeley.com/datasets/kng9rzcx3d/1)

Any additional information required to reanalyze the data reported in this paper is available from the lead contact upon request.

Experimental model and study participants details

Strains, plasmids, and growth medium and primers.

The *B. subtilis* wild-type strain 168 72 and its derivative expressing dCas9 (designated as 'wild type') and dCas9/sgRNA^{pth} (designated as 'pth-KD')³⁸ were obtained from the Bacillus Genetic Stock Center (BGSC). The rqcH gene in these strains was deleted as described below. The *B. subtilis* $\Delta rqcH$ and $\Delta rqcP$ strains 22 were provided by Vasilii Hauryliuk (Lund University). The *E. coli* strain JM109, used for expression of plasmid-encoded *B. subtilis* or *E. coli* Pth, and strain BL21(DE3) utilized for expression of recombinant *B. subtilis* RqcH and RqcP were obtained from Promega.

The plasmid pCA24N-*pth*(*Ec*) encoding the N-terminally His₆-tagged Pth was from the ASKA library ⁷⁹. The plasmids pET24d-rqcH-HTF and pET24d-rqcP-TEV-His₆ encoding recombinant RqcH and RqcP proteins were provided by Vasilii Hauryliuk (Lund University). The plasmid pLAS encoding the LepB-ADR1a-SecM sequence ⁴⁴ was provided by Gunnar von Heijne (Stockholm University). The plasmid pCA24N-*pth*(*Bs*) encoding N-terminally His₆-tagged *B. subtilis* Pth was prepared in this study.

The lysogeny broth (LB) medium [1% yeast extract, 0.5% tryptone, 1% NaCl (all w/v)] was used for growth of B. subtilis and E. coli cells.

The sequences of all oligonucleotides are specified in Table S2, the relevant sequences of the templates used for in vitro translation are shown in Table S3.

Method details

DNA manipulations

Construction of the pCA24N-pth(Bs) plasmid

All PCR reactions were performed using Phusion®High-Fidelity DNA polymerase (New England Biolabs) and PCR products were purified using PCR-purification kit (Zymo Research).

The *B. subtilis pth* gene was PCR-amplified from chromosomal DNA of the strain 168 using a mixture of four primers: Fwd-PTH_{Bs}-1 (0.05 μ M), Fwd-PTH_{Bs}-2 (0.5 μ M), Rev-PTH_{Bs}-1 (0.05 μ M), and Rev-PTH_{Bs}-2 (0.5 μ M). The amplified gene was used to replace the *E. coli pth* gene in the pCA24N-*pth*(*Ec*) plasmid by Gibson assembly ⁸⁷.

Constructing DNA templates for in vitro transcription-translation

DNA templates for in vitro transcription-translation specifying non-stop mRNAs encoding firefly luciferase (Luc) (untailed or C-terminally tailed) were prepared by PCR-amplifying the luc gene from the pBESTlucTM plasmid (Promega) using primers Fwd-T7-Luc (0.5 μ M), Fwd-Luc (0.05 μ M), and 0.5 μ M of one of the specific reverse primers designed to obtain luciferase proteins with the desired C-terminal tails (Table S2).

DNA templates for non-stop mRNAs encoding the peptides with the ADR1a domain were prepared in two consecutive PCR reactions. First, the ADR1a-encoding sequence was amplified from plasmid LepB-ADR1a-SecM ⁴⁴ using forward primer Fwd-ADR1a and one of the specific Rev-ADR1a reverse primers to obtain the desired linker sequence. The resultant DNA products were then used as templates for the second round of PCR using Fwd-T7-ADR1a, introducing the T7 RNA polymerase promoter and the ribosome binding site, and one of the specific SecM reverse primers (Rev-SecM, Rev-SecM-A₃ or Rev-SecM-A₇) designed to obtain ADR1a-containing peptide with the desired C-terminal tails (Table S2).

Phylogenetic analysis.

Representative sequences of RqcP and Hsp15 were obtained from a previous phylogenetic study (the mmc3 dataset) and aligned with MAFFT L-INS-i version 7.453 ⁸⁰. Hidden Markov Models (HMMs) profiles were built using the alignments with HMMER v3.3.2 hmmbuild.

The proteome from complete bacterial reference genomes (May 4, 2023) were downloaded from NCBP FTP. RqcP and Hsp15 homologues were identified using the HMMs profiles with HMMER v3.3.2 hmmscan with an E value cut-off of 1e⁻¹⁰. Sequences were aligned with MAFFT L-INS-i version 7.453, with alignment positions with >50% gaps removed using TrimAl v1.2 ⁸¹.

Phylogenetic analysis was executed using IQ-TREE v1.6.12 ⁸² (http://iqtree.cibiv.univie.ac.at/,) with default parameters and 1000 ultrafast bootstrap replicates ⁸⁸. Within the analysis, 'LG + I + G' was automatically selected and used as the best-fit substitution model. JalView v.2.11.2.0 ⁸³ and FigTree v.1.4.4 (https://github.com/rambaut/figtree/) were used respectively for alignment and phylogenetic tree visualization.

Gene distance and neighborhood analysis.

Homologues from Pth and RqcH were identified using HMMER v3.3.2 Jackhmmer with a maximum number of 100 iterations and an E value cut-off of $1e^{-10}$. Gene distance, defined as the number of coding genes between rqcP and pth, was determined from the gtf genome files. Gene neighborhood analysis was performed using FlaGs ⁸⁴ (https://github.com/GCA-VH-lab/FlaGs2) using Pth as query with 11 flanking genes. R version 4.2.2 was used to create and perform the gene distance distribution figures and statistical analyses.

Construction of B. subtilis strains

To delete the *rqcH* gene, the dCas9 (wild type) and dCas9/sgRNA^{pth} (*pth*-KD) *B. subtilis* strains were transformed according to the protocol described in ⁸⁹ with a linear DNA amplified from the genome of the *B. subtilis rqcH::spc* strain ²² using primers Fwd-RqcH and Rev-RqcH. Transformants were selected on LB agar plates containing spectinomycin (100 μg/mL) and the deletion of the *rqcH* gene in the recipient cells was confirmed by PCR.

Preparation of B. subtilis lysates.

Overnight cultures of *B. subtilis* cells were inoculated 1:1000 into 25 mL of fresh LB medium (containing or not 1% xylose) and grown at 37°C. Upon reaching exponential phase ($A_{600} \sim 0.7$), cultures were rapidly cooled down by adding equal volume of ice and cells were harvested by centrifugation at 4°C for 5 min at 5,500 rpm in JA-25.50 rotor (Beckman). Cell pellets were resuspended in 0.25 mL of lysis buffer (50 mM HEPES-KOH, pH 7.0, 100 mM NaCl, 10 mM MgCl₂, 5 mM CaCl₂, 0.4% Triton X-100, 0.1% NP-40) containing 1 mg/mL lysozyme, 40 units of DNase I and 0.8% Complete Protease Inhibitor cocktail. Cell suspension was mixed with 290 mg of 0.1 mm zirconium beads (BioSpec Products) and lysed using Fast-Prep homogenizer for 1 min at 6.5 m/s (BaneBio). The resultant lysates were clarified by centrifugation at 4°C for 10 min at 21,000 rcf in the Eppendorf microcentrifuge, the supernatants were collected, flash frozen in liquid nitrogen and stored at -80°C. Prior to use, the lysates were diluted with the cold lysis buffer to A_{260} of 1.0.

Preparation of 50S-NCC.

The complexes of 70S ribosomes carrying different stalled peptidyl-tRNAs were generated by in vitro transcription-translation of the corresponding DNA templates in the PURExpress Δ ribosome cell-free system (New England Biolabs). The ribosomes were supplemented to a final concentration of 3.6 µM. Ribosomes from B. subtilis strain 168 or E. coli strain SQ171 pAM55-2 ⁷⁸ were isolated as described ⁹⁰. To generate stalled ribosomes carrying radiolabeled nascent peptides, the reactions contained 50 µM of unlabeled methionine and 1.1 µCi/µL of EasyTag Express ³⁵S Protein Labeling Mix (PerkinElmer) with a specific activity of 1175 Ci/mmol. After assembling the reaction components (final volume 50 µL), reactions were initiated by adding 0.5 ug of templates. To prevent tmRNA-mediated decay of 70S:peptidyl-tRNA complexes accumulated during transcription-translation, all reactions were supplemented with 5 µM of antitmRNA DNA oligonucleotide (Table S2). After 1h incubation at 37°C (for the reactions with B. subtilis ribosomes) or at 30°C (for the reactions with E. coli ribosomes), samples were diluted with an equal volume (50 µL) of cold 10/100 buffer containing 20 mM HEPES-KOH, pH 7.5, 10 mM Mg(OAc)₂, 100 mM KOAc, 2 mM DTT and loaded onto 5-20% sucrose gradient in ribosome dissociation buffer (20 mM HEPES-KOH pH 7.5, 1 mM Mg(OAc)₂, 100 mM KOAc, 2 mM DTT). Gradients were centrifuged at 40,000 rpm for 2.5 hours at 4°C in a SW41Ti rotor and fractionated

using Gradient Fractionator (BioComp Instruments). Fractions containing the Luc-based 50S-NCC were collected, flash frozen in liquid nitrogen, and stored at -80°C. The similarly isolated 50S-NCCs from the reactions generating [35 S]-labeled nascent ADR1a peptides, were pelleted by centrifugation at 100,000 rpm for 5 h in a S110AT rotor (Hitachi). The pellets were resuspended in 25 μ L of 10/100 buffer, flash frozen in liquid nitrogen, and stored at -80°C.

Protein expression and purification

B. subtilis RqcH and RqcP were expressed in the *E. coli* BL21(DE3) strain and purified generally following the described procedure 43 with minor modifications. Specifically, for RqcP purification, fractions containing RqcP eluted from a 5 mL HisTrap HP column were combined and dialyzed against buffer 25 mM HEPES-KOH, pH 7.5, 5 mM MgCl₂, 500 mM KCl, 10% glycerol, and 1 mM β-mercaptoethanol. The proteins was aliquoted, flash frozen in liquid nitrogen, and stored at -80°C.

B. subtilis and *E. coli* Pth proteins were expressed in *E. coli* JM109 cells. Colonies of the freshly transformed cells were inoculated into 1 L LB medium containing 20 μg/mL chloramphenicol and grown at 37°C with intense agitation. When the cultures reached A₆₀₀ of 0.5, IPTG was added to the final concentration of 1 mM and growth continued for an additional 2 h at 37°C. Cells were harvested by centrifugation, resuspended in 30 mL binding buffer (20 mM HEPES-KOH, pH 7.5, 10 mM Mg(OAc)₂, 100 mM KOAc, and 0.5 mM DTT) supplemented with 1% Complete Protease Inhibitor cocktail, and lysed by one passage through a French press (SLM Aminco, Inc). Cell debris was removed by centrifugation at 17,000 rpm for 30 min at 4°C in a JA-25.50 rotor (Beckman Coulter). Clarified lysates were filtered through a 0.2 μm syringe filter and loaded onto a 5 mL HisTrap HP column (Cytiva) pre-equilibrated in binding buffer. The column was washed with 5 column volumes of binding buffer and then with 5 volumes of the same buffer supplemented with 20 mM imidazole. The Pth was eluted with a linear gradient of imidazole (20-500 mM) in binding buffer. Pth-containing fractions were combined and dialyzed against either 10/100 buffer (for *B. subtilis* Pth) or 10 mM Tris-HCl, pH 7.5 (for *E. coli* Pth). After dialysis, proteins were aliquoted, flash frozen in liquid nitrogen and stored at -80°C.

Luciferase release assay

Aliquots (25 μ L) of Luc-based 50S-NCC were thawed on ice and mixed with an equal volume of the Assay Buffer (20 mM HEPES-KOH pH 7.5, 19 mM Mg(OAc)₂, 100 mM KOAc, 2 mM DTT, 2 mM ATP and 0.2 mM D-luciferin). The mixtures (50 μ L) were transferred into wells of 384-well black/clear assay plates (Falcon) and placed into a microplate reader (Infinite M200Pro, Tecan) pre-set at 30°C. After recording the background luminescence for 2 min, the release of nascent luciferase from 50S-NCC was initiated by addition of 1 μ L of bacterial lysate or purified Pth (0.15 μ M). The time course of light emission reflecting accumulation of enzymatically active released protein was recorded over time.

The tailing/release reactions on Luc-tRNA 50S-NCCs were carried out at 30°C in the Buffer 20 mM HEPES-KOH pH 7.5, 10 mM Mg(OAc)₂, 100 mM KOAc, 2 mM DTT, 2 mM ATP supplemented with purified *B. subtilis* or *E. coli* components added to the following final concentrations: 3 nM Pth (*B. subtilis*), 30 nM RqcH (*B. subtilis*), 30 nM RqcP (*B. subtilis*), 120 nM alanyl-tRNA synthetase (*E. coli*), 50 μg/mL tRNA^{Ala} (*E. coli*), and 0.2 mM L-alanine. After the specified times, puromycin was added to the reactions to the final concentration of 0.5 mM to release residual nascent Luc from 50S-NCC.

Pth-mediated pept-tRNAs hydrolysis in ADR1a-containing 50S-NCC.

For Pth-mediated pept-tRNA hydrolysis, 33 pmol of 50S-NCC carrying [³⁵S]-labeled ADR1a nascent peptides were placed in 5 μL of 10/100 buffer containing 0.1 mM ZnCl₂ or TPEN (*N*,*N*,*N*',*N*'-tetrakis(2-pyridinylmethyl)-1,2-ethanediamine). After incubation for 5 min at 30°C, 0.5 μL of 3 μM Pth was added to the mixtures and incubation continued for 15 min. The reactions were then mixed with 5 μL of 2x Tricine loading buffer (Bio-Rad) and resolved using Bis-Tris SDS-PAGE (https://openwetware.org/wiki/Sauer:bis-Tris_SDS-PAGE,_the_very_best) to prevent spontaneous hydrolysis of pept-tRNAs ester bonds. Gels were stained, dried and exposed overnight to a phosphorimager screen. Radioactivity was visualized in the Typhoon Trio phosphorimager (GE Healthcare). The intensity of the bands was quantified using ImageJ ⁸⁶.

Hydrolysis of ErmDL-tRNA in cell lysate

Four pmol (100 ng) of ErmDL-tRNA 48 were incubated in 10 μ L of 10/100 buffer with 0.5 μ L of the *B. subtilis* lysate prepared as described above. After incubation for 15 min at 30°C, the

reactions were mixed with 10 μ L of 2x Tricine loading buffer (Bio-Rad) and resolved in Bis-Tris SDS gel ((https://openwetware.org/wiki/Sauer:bis-Tris_SDS-PAGE,_the_very_best). Gels were stained with ethidium bromide and tRNA bands were visualized in ChemiDoc MP Imaging System (Bio-Rad).

Quantification and statistical analysis

Statistical significance was assigned using Prism Version 9 (GraphPad). Each dot represents an individual experiment. The specific tests, number of experiments and dispersion and precision measures are indicated in the Figure legends.

SUPPLEMENTAL TABLE TITLES

Supplemental Table S1. Gene neighborhood of the closely spaced *rqcP* and *pth* genes in the *rqcH*-positive bacteria, related to Figure 1.

Supplemental Table S2. DNA oligonucleotides used in the study, related to STAR Methods

Supplemental Table S3. Amino acid sequences of the reporter constructs used in the study, related to Figures 2-5.

REFERENCES

- 1. Filbeck, S., Cerullo, F., Pfeffer, S., and Joazeiro, C.A.P. (2022). Ribosome-associated quality-control mechanisms from bacteria to humans. Mol Cell 82, 1451-1466.
- 2. Muller, C., Crowe-McAuliffe, C., and Wilson, D.N. (2021). Ribosome rescue pathways in bacteria. Front Microbiol *12*, 652980.
- 3. Howard, C.J., and Frost, A. (2021). Ribosome-associated quality control and CAT tailing. Crit Revs Biochem Molec Biol *56*, 603-620.
- 4. Becker, T., Franckenberg, S., Wickles, S., Shoemaker, C.J., Anger, A.M., Armache, J.P., Sieber, H., Ungewickell, C., Berninghausen, O., Daberkow, I., et al. (2012). Structural basis of highly conserved ribosome recycling in eukaryotes and archaea. Nature 482, 501-506.
- 5. Pisareva, V.P., Skabkin, M.A., Hellen, C.U., Pestova, T.V., and Pisarev, A.V. (2011). Dissociation by Pelota, Hbs1 and ABCE1 of mammalian vacant 80S ribosomes and stalled elongation complexes. EMBO J *30*, 1804-1817.
- 6. Franckenberg, S., Becker, T., and Beckmann, R. (2012). Structural view on recycling of archaeal and eukaryotic ribosomes after canonical termination and ribosome rescue. Curr Opin Struct Biol 22, 786-796.
- 7. Buskirk, A.R., and Green, R. (2017). Ribosome pausing, arrest and rescue in bacteria and eukaryotes. Philos Trans R Soc Lond B Biol Sci *372*, 20160183.
- 8. Joazeiro, C.A.P. (2019). Mechanisms and functions of ribosome-associated protein quality control. Nature reviews. Mol Cell Biol *20*, 368-383.
- 9. Lyumkis, D., Oliveira dos Passos, D., Tahara, E.B., Webb, K., Bennett, E.J., Vinterbo, S., Potter, C.S., Carragher, B., and Joazeiro, C.A. (2014). Structural basis for translational surveillance by the large ribosomal subunit-associated protein quality control complex. Proc Natl Acad Sci USA *111*, 15981-15986.
- 10.Shen, P.S., Park, J., Qin, Y., Li, X., Parsawar, K., Larson, M.H., Cox, J., Cheng, Y., Lambowitz, A.M., Weissman, J.S., et al. (2015). Protein synthesis. Rqc2p and 60S ribosomal subunits mediate mRNA-independent elongation of nascent chains. Science *347*, 75-78.
- 11. Kostova, K.K., Hickey, K.L., Osuna, B.A., Hussmann, J.A., Frost, A., Weinberg, D.E., and Weissman, J.S. (2017). CAT-tailing as a fail-safe mechanism for efficient degradation of stalled nascent polypeptides. Science *357*, 414-417.
- 12. Osuna, B.A., Howard, C.J., Kc, S., Frost, A., and Weinberg, D.E. (2017). In vitro analysis of RQC activities provides insights into the mechanism and function of CAT tailing. eLife 6. 10.7554
- 13. Bengtson, M.H., and Joazeiro, C.A. (2010). Role of a ribosome-associated E3 ubiquitin ligase in protein quality control. Nature *467*, 470-473.

- 14. Brandman, O., Stewart-Ornstein, J., Wong, D., Larson, A., Williams, C.C., Li, G.W., Zhou, S., King, D., Shen, P.S., Weibezahn, J., et al. (2012). A ribosome-bound quality control complex triggers degradation of nascent peptides and signals translation stress. Cell *151*, 1042-1054.
- 15. Defenouillere, Q., Yao, Y., Mouaikel, J., Namane, A., Galopier, A., Decourty, L., Doyen, A., Malabat, C., Saveanu, C., Jacquier, A., and Fromont-Racine, M. (2013). Cdc48-associated complex bound to 60S particles is required for the clearance of aberrant translation products. Proc Natl Acad Sci USA *110*, 5046-5051.
- 16. Thrun, A., Garzia, A., Kigoshi-Tansho, Y., Patil, P.R., Umbaugh, C.S., Dallinger, T., Liu, J., Kreger, S., Patrizi, A., Cox, G.A., et al. (2021). Convergence of mammalian RQC and C-end rule proteolytic pathways via alanine tailing. Mol Cell. *81*, 12112-2122
- 17. Patil, P.R., Burroughs, A.M., Misra, M., Cerullo, F., Dikic, I., Aravind, L., and Joazeiro, C.A.P. (2023). Mechanism and evolutionary origins of Alanine-tail C-degron recognition by E3 ligases Pirh2 and CRL2-KLHDC10. bioRxiv. 10.1101/2023.05.03.539038.
- 18. Lytvynenko, I., Paternoga, H., Thrun, A., Balke, A., Muller, T.A., Chiang, C.H., Nagler, K., Tsaprailis, G., Anders, S., Bischofs, I., et al. (2019). Alanine tails signal proteolysis in bacterial Ribosome-Associated Quality Control. Cell *178*, 76-90 e22.
- 19. Cerullo, F., Filbeck, S., Patil, P.R., Hung, H.C., Xu, H., Vornberger, J., Hofer, F.W., Schmitt, J., Kramer, G., Bukau, B., et al. (2022). Bacterial ribosome collision sensing by a MutS DNA repair ATPase paralogue. Nature *603*, 509-514.
- 20. Park, E., Mackens-Kiani, T., Berhane, R., Esser, H., Erdenebat, C., Burroughs, A.M., Berninghausen, O., Aravind, L., Beckmann, R., Green, R., and Buskirk, A.R. (2023). B. subtilis MutS2 splits stalled ribosomes into subunits without mRNA cleavage. bioRxiv. 10.1101/2023.05.05.539626.
- 21. Filbeck, S., Cerullo, F., Paternoga, H., Tsaprailis, G., Joazeiro, C.A.P., and Pfeffer, S. (2021). Mimicry of canonical translation elongation underlies alanine tail synthesis in RQC. Mol Cell 81, 104-114
- 22. Crowe-McAuliffe, C., Takada, H., Murina, V., Polte, C., Kasvandik, S., Tenson, T., Ignatova, Z., Atkinson, G.C., Wilson, D.N., and Hauryliuk, V. (2021). Structural basis for bacterial ribosome-associated quality control by RqcH and RqcP. Mol Cell 81, 115-126.
- 23. Chadani, Y., Niwa, T., Izumi, T., Sugata, N., Nagao, A., Suzuki, T., Chiba, S., Ito, K., and Taguchi, H. (2017). Intrinsic ribosome destabilization underlies translation and provides an organism with a strategy of environmental sensing. Mol Cell *68*, 528-539.
- 24. Chadani, Y., Sugata, N., Niwa, T., Ito, Y., Iwasaki, S., and Taguchi, H. (2021). Nascent polypeptide within the exit tunnel stabilizes the ribosome to counteract risky translation. EMBO J 40, e108299.

- 25. Rudra, P., Hurst-Hess, K.R., Cotten, K.L., Partida-Miranda, A., and Ghosh, P. (2020). Mycobacterial HflX is a ribosome splitting factor that mediates antibiotic resistance. Proc Natl Acad Sci USA *117*, 629-634.
- 26. Jiang, L., Schaffitzel, C., Bingel-Erlenmeyer, R., Ban, N., Korber, P., Koning, R.I., de Geus, D.C., Plaisier, J.R., and Abrahams, J.P. (2009). Recycling of aborted ribosomal 50S subunit-nascent chain-tRNA complexes by the heat shock protein Hsp15. J Mol Biol *386*, 1357-1367.
- 27. Safdari, H.A., Kasvandik, S., Polte, C., Ignatova, Z., Tenson, T., and Wilson, D.N. (2022). Structure of Escherichia coli heat shock protein Hsp15 in complex with the ribosomal 50S subunit bearing peptidyl-tRNA. Nucleic Acids Res 50, 12515-12526.
- 28. Sengupta, S., Mondal, A., Dutta, D., and Parrack, P. (2018). HflX protein protects *Escherichia coli* from manganese stress. J Biosci *43*, 1001-1013.
- 29. Bhattacharjee, S., Feng, X., Maji, S., Brown, Z.P., and Frank, J. (2023). Time resolution in cryo-EM using a novel PDMS-based microfluidic chip assembly and its application to the study of HflX-mediated ribosome recycling. bioRxiv. 10.1101/2023.01.25.525430.
- 30. Verma, R., Reichermeier, K.M., Burroughs, A.M., Oania, R.S., Reitsma, J.M., Aravind, L., and Deshaies, R.J. (2018). Vms1 and ANKZF1 peptidyl-tRNA hydrolases release nascent chains from stalled ribosomes. Nature *557*, 446-451.
- 31. Yip, M.C.J., Keszei, A.F.A., Feng, Q., Chu, V., McKenna, M.J., and Shao, S. (2019). Mechanism for recycling tRNAs on stalled ribosomes. Nat Struct Mol Biol *26*, 343-349.
- 32. Su, T., Izawa, T., Thoms, M., Yamashita, Y., Cheng, J., Berninghausen, O., Hartl, F.U., Inada, T., Neupert, W., and Beckmann, R. (2019). Structure and function of Vms1 and Arb1 in RQC and mitochondrial proteome homeostasis. Nature *570*, 538-542.
- 33. Kuroha, K., Zinoviev, A., Hellen, C.U.T., and Pestova, T.V. (2018). Release of ubiquitinated and non-ubiquitinated nascent chains from stalled mammalian ribosomal complexes by ANKZF1 and Ptrh1. Mol Cell 72, 286-302.
- 34. Svetlov, M.S. (2021). Ribosome-associated quality control in bacteria. Biokhimiia *86*, 942-951.
- 35. Menninger, J.R. (1976). Peptidyl transfer RNA dissociates during protein synthesis from ribosomes of *Escherichia coli*. J Biol Chem *251*, 3392-3398.
- 36.Nagao, A., Nakanishi, Y., Yamaguchi, Y., Mishina, Y., Karoji, M., Toya, T., Fujita, T., Iwasaki, S., Miyauchi, K., Sakaguchi, Y., and Suzuki, T. (2023). Quality control of protein synthesis in the early elongation stage. Nat Commun *14*, 2704. 10.1038/s41467-023-38077-5.
- 37. Overbeek, R., Fonstein, M., D'Souza, M., Pusch, G.D., and Maltsev, N. (1999). The use of gene clusters to infer functional coupling. Proc Natl Acad Sci USA *96*, 2896-2901.

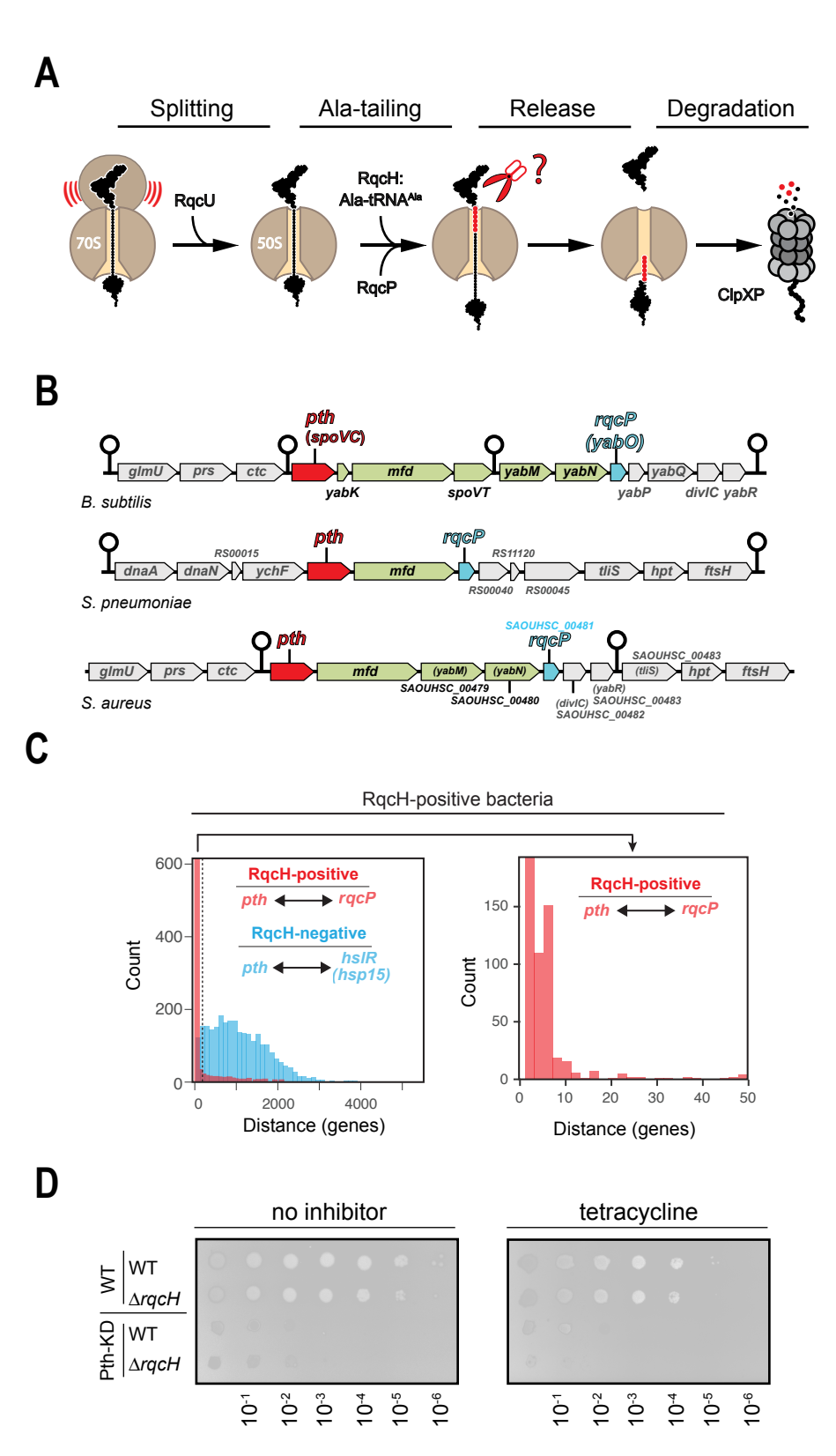
- 38. Peters, J.M., Colavin, A., Shi, H., Czarny, T.L., Larson, M.H., Wong, S., Hawkins, J.S., Lu, C.H.S., Koo, B.M., Marta, E., et al. (2016). A comprehensive, CRISPR-based functional analysis of essential genes in bacteria. Cell *165*, 1493-1506.
- 39. Saito, K., Kratzat, H., Campbell, A., Buschauer, R., Burroughs, A.M., Berninghausen, O., Aravind, L., Green, R., Beckmann, R., and Buskirk, A.R. (2022). Ribosome collisions induce mRNA cleavage and ribosome rescue in bacteria. Nature *603*, 503-508.
- 40. Kolb, V.A., Makeyev, E.V., and Spirin, A.S. (1994). Folding of firefly luciferase during translation in a cell-free system. EMBO J *13*, 3631-3637.
- 41. Svetlov, M.S., Kommer, A., Kolb, V.A., and Spirin, A.S. (2006). Effective cotranslational folding of firefly luciferase without chaperones of the Hsp70 family. Protein Sci *15*, 242-247.
- 42. Aviner, R. (2020). The science of puromycin: From studies of ribosome function to applications in biotechnology. Comput Struct Biotechnol J 18, 1074-1083.
- 43. Takada, H., Crowe-McAuliffe, C., Polte, C., Sidorova, Z.Y., Murina, V., Atkinson, G.C., Konevega, A.L., Ignatova, Z., Wilson, D.N., and Hauryliuk, V. (2021). RqcH and RqcP catalyze processive poly-alanine synthesis in a reconstituted ribosome-associated quality control system. Nucleic Acids Res *49*, 8355-8369.
- 44. Nilsson, O.B., Hedman, R., Marino, J., Wickles, S., Bischoff, L., Johansson, M., Muller-Lucks, A., Trovato, F., Puglisi, J.D., O'Brien, E.P., et al. (2015). Cotranslational protein folding inside the ribosome exit tunnel. Cell Rep *12*, 1533-1540.
- 45. Schmeing, T.M., Huang, K.S., Kitchen, D.E., Strobel, S.A., and Steitz, T.A. (2005). Structural insights into the roles of water and the 2' hydroxyl of the P site tRNA in the peptidyl transferase reaction. Mol Cell *20*, 437-448.
- 46. Svidritskiy, E., Ling, C., Ermolenko, D.N., and Korostelev, A.A. (2013). Blasticidin S inhibits translation by trapping deformed tRNA on the ribosome. Proc Natl Acad Sci USA *110*, 12283-12288.
- 47. Tsai, K., Stojkovic, V., Lee, D.J., Young, I.D., Szal, T., Klepacki, D., Vazquez-Laslop, N., Mankin, A.S., Fraser, J.S., and Fujimori, D.G. (2022). Structural basis for context-specific inhibition of translation by oxazolidinone antibiotics. Nat Struct Mol Biol *29*, 162-171.
- 48. Syroegin, E.A., Flemmich, L., Klepacki, D., Vazquez-Laslop, N., Micura, R., and Polikanov, Y.S. (2022). Structural basis for the context-specific action of the classic peptidyl transferase inhibitor chloramphenicol. Nat Struct Mol Biol *29*, 152-161.
- 49. Moazed, D., and Noller, H.F. (1991). Sites of interaction of the CCA end of peptidyl-tRNA with 23S rRNA. Proc Natl Acad Sci USA 88, 3725-3728.
- 50. Samaha, R.R., Green, R., and Noller, H.F. (1995). A base pair between tRNA and 23S rRNA in the peptidyl transferase centre of the ribosome. Nature *377*, 309-314.

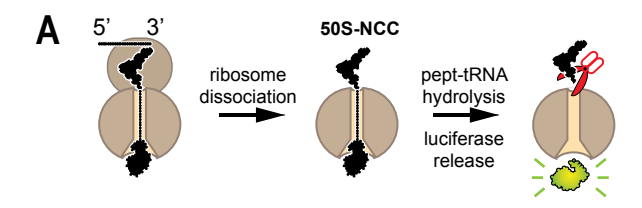
- 51. Wilson, D.N., and Beckmann, R. (2011). The ribosomal tunnel as a functional environment for nascent polypeptide folding and translational stalling. Curr Opin Struct Biol *21*, 274-282.
- 52. Kossel, H. (1970). Purification and properties of peptidyl-tRNA hydrolase from Escherichia coli. Biochimica et biophysica acta *204*, 191-202.
- 53. van der Stel, A.X., Gordon, E.R., Sengupta, A., Martinez, A.K., Klepacki, D., Perry, T.N., Herrero Del Valle, A., Vazquez-Laslop, N., Sachs, M.S., Cruz-Vera, L.R., and Innis, C.A. (2021). Structural basis for the tryptophan sensitivity of TnaC-mediated ribosome stalling. Nat commun *12*, 5340.
- 54. Beckert, B., Leroy, E.C., Sothiselvam, S., Bock, L.V., Svetlov, M.S., Graf, M., Arenz, S., Abdelshahid, M., Seip, B., Grubmuller, H., et al. (2021). Structural and mechanistic basis for translation inhibition by macrolide and ketolide antibiotics. Nat Commun *12*, 4466.
- 55. Li, W., Chang, S.T., Ward, F.R., and Cate, J.H.D. (2020). Selective inhibition of human translation termination by a drug-like compound. Nat Commun 11, 4941.
- 56. Huter, P., Arenz, S., Bock, L.V., Graf, M., Frister, J.O., Heuer, A., Peil, L., Starosta, A.L., Wohlgemuth, I., Peske, F., et al. (2017). Structural basis for polyproline-mediated ribosome stalling and rescue by the translation elongation factor EF-P. Mol Cell *68*, 515-527.
- 57. Chandrasekaran, V., Juszkiewicz, S., Choi, J., Puglisi, J.D., Brown, A., Shao, S., Ramakrishnan, V., and Hegde, R.S. (2019). Mechanism of ribosome stalling during translation of a poly(A) tail. Nat Struct Mol Biol *26*, 1132-1140.
- 59. Menninger, J.R., Mulholland, M.C., and Stirewalt, W.S. (1970). Peptidyl-tRNA hydrolase and protein chain termination. Biochim Biophys Acta *217*, 496-511.
- 59. Menninger, J.R. (1979). Accumulation of peptidyl tRNA is lethal to *Escherichia coli*. J Bacteriol *137*, 694-696.
- 60. Vivanco-Dominguez, S., Bueno-Martinez, J., Leon-Avila, G., Iwakura, N., Kaji, A., Kaji, H., and Guarneros, G. (2012). Protein synthesis factors (RF1, RF2, RF3, RRF, and tmRNA) and peptidyl-tRNA hydrolase rescue stalled ribosomes at sense codons. J Mol Biol *417*, 425-439.
- 61. Korber, P., Stahl, J.M., Nierhaus, K.H., and Bardwell, J.C. (2000). Hsp15: a ribosome-associated heat shock protein. EMBO J 19, 741-748.
- 62. Jain, N., Dhimole, N., Khan, A.R., De, D., Tomar, S.K., Sajish, M., Dutta, D., Parrack, P., and Prakash, B. (2009). *E. coli* HflX interacts with 50S ribosomal subunits in presence of nucleotides. Biochem Biophys Res Commun *379*, 201-205.
- 63. Zhang, Y., Mandava, C.S., Cao, W., Li, X., Zhang, D., Li, N., Zhang, Y., Zhang, X., Qin, Y., Mi, K., et al. (2015). HflX is a ribosome-splitting factor rescuing stalled ribosomes under stress conditions. Nat Struct Mol Biol *22*, 906-913.

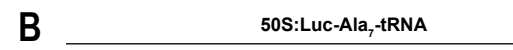
- 64. Coatham, M.L., Brandon, H.E., Fischer, J.J., Schummer, T., and Wieden, H.J. (2016). The conserved GTPase HflX is a ribosome splitting factor that binds to the E-site of the bacterial ribosome. Nucleic Acids Res *44*, 1952-1961.
- 65. Duval, M., Dar, D., Carvalho, F., Rocha, E.P.C., Sorek, R., and Cossart, P. (2018). HflXr, a homolog of a ribosome-splitting factor, mediates antibiotic resistance. Proc Natl Acad Sci USA *115*, 13359-13364.
- 66. Ramadoss, N.S., Alumasa, J.N., Cheng, L., Wang, Y., Li, S., Chambers, B.S., Chang, H., Chatterjee, A.K., Brinker, A., Engels, I.H., and Keiler, K.C. (2013). Small molecule inhibitors of trans-translation have broad-spectrum antibiotic activity. Proc Natl Acad Sci USA *110*, 10282-10287.
- 67. Aron, Z.D., Mehrani, A., Hoffer, E.D., Connolly, K.L., Srinivas, P., Torhan, M.C., Alumasa, J.N., Cabrera, M., Hosangadi, D., Barbor, J.S., et al. (2021). trans-Translation inhibitors bind to a novel site on the ribosome and clear *Neisseria gonorrhoeae* in vivo. Nat Commun *12*, 1799.
- 68. Menninger, J.R., and Otto, D.P. (1982). Erythromycin, carbomycin, and spiramycin inhibit protein synthesis by stimulating the dissociation of peptidyl-tRNA from ribosomes. Antimicrob Agents Chemother *21*, 810-818.
- 69. Menninger, J.R., and Coleman, R.A. (1993). Lincosamide antibiotics stimulate dissociation of peptidyl-tRNA from ribosomes. Antimicrob Agents Chemother *37*, 2027-2029.
- 70. Tomasi, F.G., Schweber, J.T.P., Kimura, S., Zhu, J., Cleghorn, L.A.T., Davis, S.H., Green, S.R., Waldor, M.K., and Rubin, E.J. (2023). Peptidyl tRNA hydrolase is required for robust prolyl-tRNA turnover in *Mycobacterium tuberculosis*. mBio *14*, e0346922.
- 71. Wruck, F., Tian, P., Kudva, R., Best, R.B., von Heijne, G., Tans, S.J., and Katranidis, A. (2021). The ribosome modulates folding inside the ribosomal exit tunnel. Commun Biol *4*, 523.
- 72. Kunst, F., Ogasawara, N., Moszer, I., Albertini, A.M., Alloni, G., Azevedo, V., Bertero, M.G., Bessieres, P., Bolotin, A., Borchert, S., et al. (1997). The complete genome sequence of the gram-positive bacterium *Bacillus subtilis*. Nature *390*, 249-256.
- 73. ten Broeke-Smits, N.J., Pronk, T.E., Jongerius, I., Bruning, O., Wittink, F.R., Breit, T.M., van Strijp, J.A., Fluit, A.C., and Boel, C.H. (2010). Operon structure of *Staphylococcus aureus*. Nucleic Acids Res *38*, 3263-3274.
- 74. Warrier, I., Ram-Mohan, N., Zhu, Z., Hazery, A., Echlin, H., Rosch, J., Meyer, M.M., and van Opijnen, T. (2018). The transcriptional landscape of *Streptococcus pneumoniae* TIGR4 reveals a complex operon architecture and abundant riboregulation critical for growth and virulence. PLoS Pathog *14*, e1007461.
- 75. Sohmen, D., Chiba, S., Shimokawa-Chiba, N., Innis, C.A., Berninghausen, O., Beckmann, R., Ito, K., and Wilson, D.N. (2015). Structure of the Bacillus subtilis 70S ribosome reveals the basis for species-specific stalling. Nat Commun *6*, 6941.

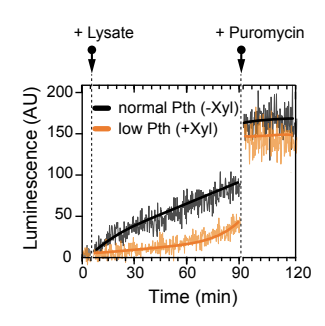
- 76. Ito, K., Murakami, R., Mochizuki, M., Qi, H., Shimizu, Y., Miura, K., Ueda, T., and Uchiumi, T. (2012). Structural basis for the substrate recognition and catalysis of peptidyl-tRNA hydrolase. Nucleic Acids Res *40*, 10521-10531.
- 77. Cruz-Vera, L.R., Toledo, I., Hernandez-Sanchez, J., and Guarneros, G. (2000). Molecular basis for the temperature sensitivity of Escherichia coli pth(Ts). J Bacteriol *182*, 1523-1528.
- 78. Orelle, C., Carlson, E.D., Szal, T., Florin, T., Jewett, M.C., and Mankin, A.S. (2015). Protein synthesis by ribosomes with tethered subunits. Nature *524*, 119-124.
- 79. Kitagawa, M., Ara, T., Arifuzzaman, M., Ioka-Nakamichi, T., Inamoto, E., Toyonaga, H., and Mori, H. (2005). Complete set of ORF clones of *Escherichia coli* ASKA library (A Complete Set of E. coli K-12 ORF Archive): Unique Resources for Biological Research. DNA Res *12*, 291-299.
- 80. Katoh, K., and Standley, D.M. (2013). MAFFT multiple sequence alignment software version 7: improvements in performance and usability. Mol Biol Evol *30*, 772-780.
- 81. Capella-Gutierrez, S., Silla-Martinez, J.M., and Gabaldon, T. (2009). trimAl: a tool for automated alignment trimming in large-scale phylogenetic analyses. Bioinformatics *25*, 1972-1973.
- 82. Nguyen, L.T., Schmidt, H.A., von Haeseler, A., and Minh, B.Q. (2015). IQ-TREE: a fast and effective stochastic algorithm for estimating maximum-likelihood phylogenies. Mol Biol Evol *32*, 268-274.
- 83. Waterhouse, A.M., Procter, J.B., Martin, D.M., Clamp, M., and Barton, G.J. (2009). Jalview Version 2--a multiple sequence alignment editor and analysis workbench. Bioinformatics *25*, 1189-1191.
- 84. Saha, C.K., Sanches Pires, R., Brolin, H., Delannoy, M., and Atkinson, G.C. (2021). FlaGs and webFlaGs: discovering novel biology through the analysis of gene neighbourhood conservation. Bioinformatics *37*, 1312-1314.
- 85. Pettersen, E.F., Goddard, T.D., Huang, C.C., Couch, G.S., Greenblatt, D.M., Meng, E.C., and Ferrin, T.E. (2004). UCSF Chimera--a visualization system for exploratory research and analysis. J Comp Chem *25*, 1605-1612.
- 86. Schneider, C.A., Rasband, W.S., and Eliceiri, K.W. (2012). NIH Image to ImageJ: 25 years of image analysis. Nat Methods *9*, 671-675.
- 87. Gibson, D.G., Young, L., Chuang, R.Y., Venter, J.C., Hutchison, C.A., 3rd, and Smith, H.O. (2009). Enzymatic assembly of DNA molecules up to several hundred kilobases. Nature methods *6*, 343-345.
- 88. Hoang, D.T., Chernomor, O., von Haeseler, A., Minh, B.Q., and Vinh, L.S. (2018). UFBoot2: Improving the ultrafast bootstrap approximation. Mol Biol Evol *35*, 518-522.

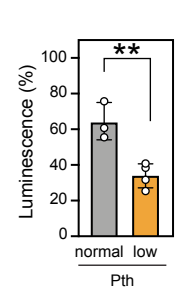
- 89. Kunst, F., and Rapoport, G. (1995). Salt stress is an environmental signal affecting degradative enzyme synthesis in Bacillus subtilis. J Bacteriol *177*, 2403-2407.
- 90. Shimizu, Y., Inoue, A., Tomari, Y., Suzuki, T., Yokogawa, T., Nishikawa, K., and Ueda, T. (2001). Cell-free translation reconstituted with purified components. Nat Biotechnol *19*, 751-755.

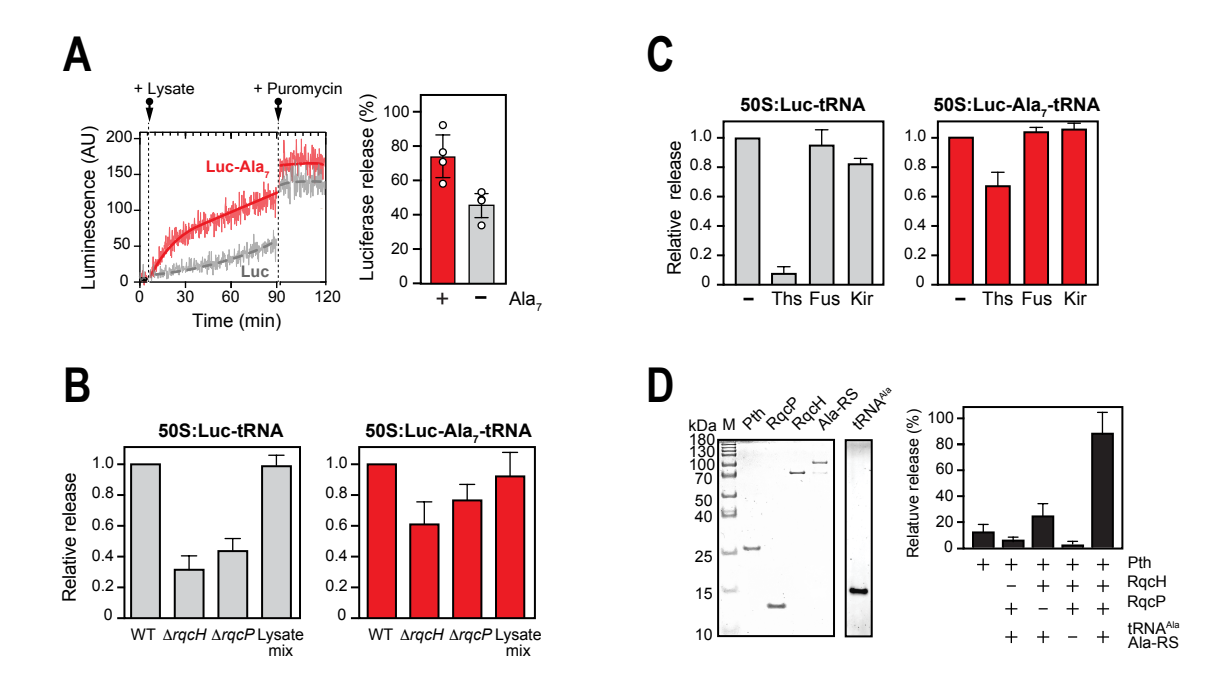


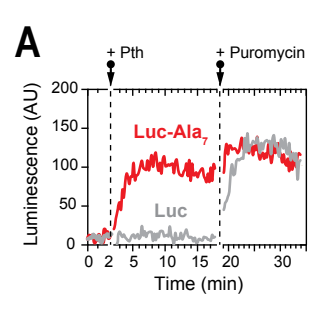


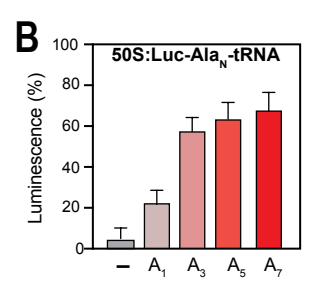


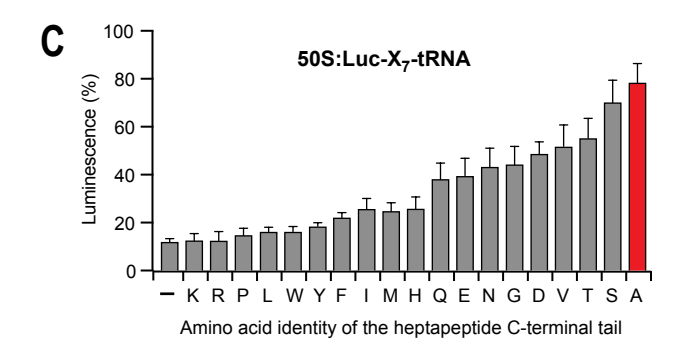


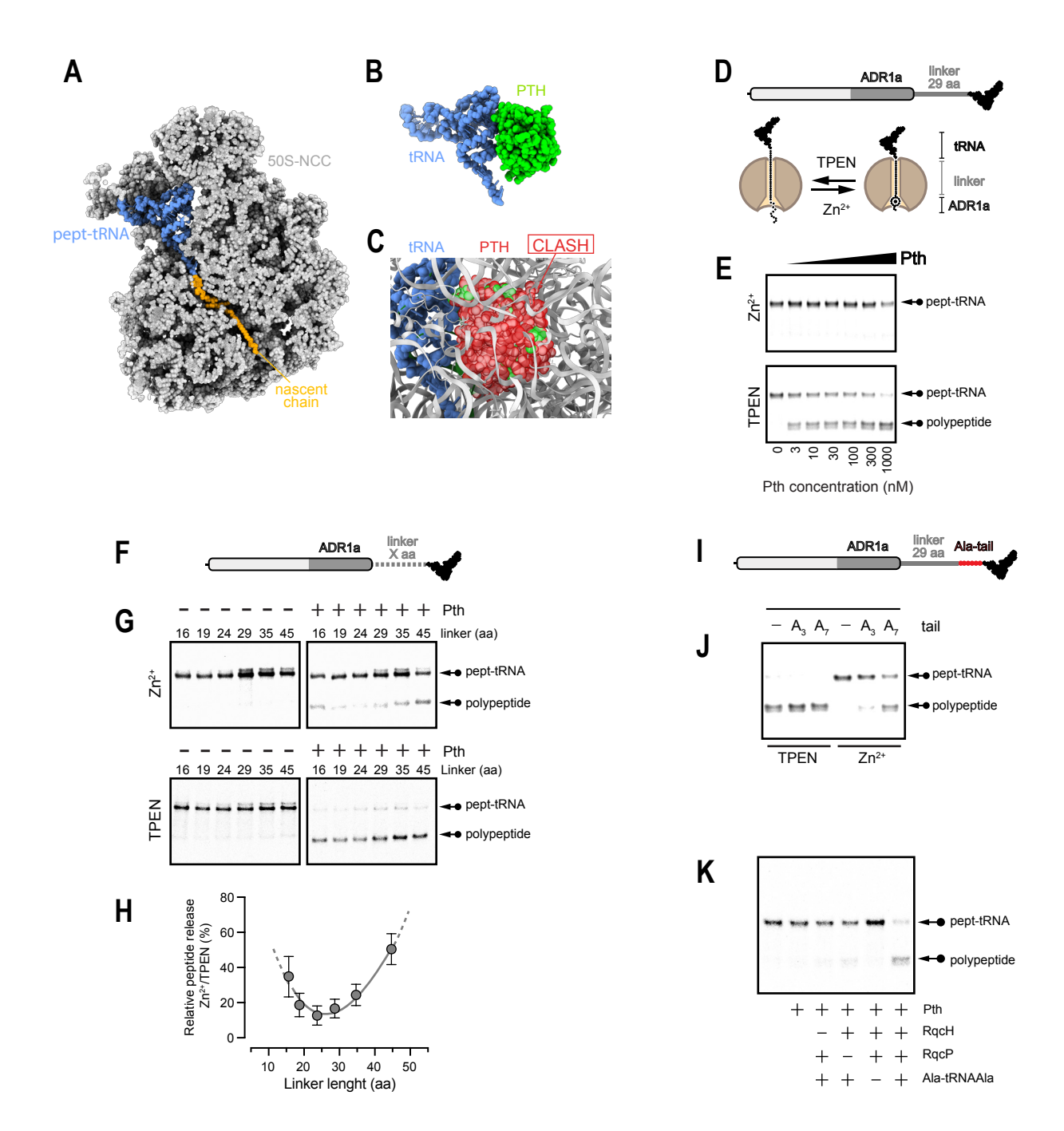




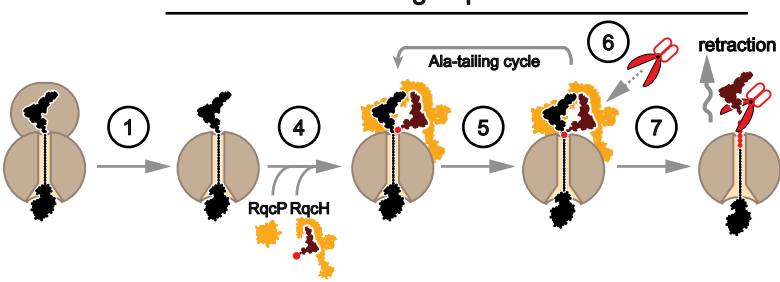








Tailing-independent Tailing-dependent Tailing-dependent



SUPPLEMENTAL INFORMATION

Peptidyl-tRNA hydrolase is the nascent chain release factor in bacterial ribosome-associated quality control

Maxim S. Svetlov, Clémence F. Dunand, Jose A. Nakamoto, Gemma C. Atkinson, Haaris A. Safdari, Daniel N. Wilson, Nora Vázquez-Laslop, Alexander S. Mankin

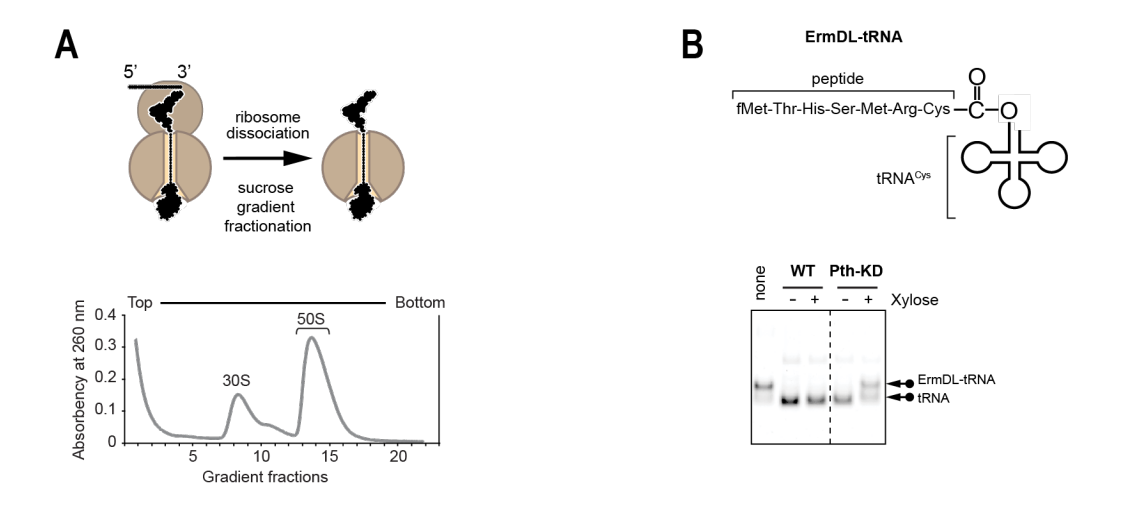


Figure S1. Preparation of 50S-Luc-tRNA complexes and hydrolysis of ribosome-free peptidyl-tRNA in *B. subtilis* lysates (Related to Figures 2-4). (A) Following in vitro translation of a non-stop template encoding Luc-A₇, ribosomes were dissociated into subunits by reducing concentration of Mg²⁺ to 1 mM, and 50S-NCC were isolated by sucrose gradient centrifugation. The fractions containing 50S particles were collected and used for the luciferase release assays. (B) Top, the model pept-tRNA prepared by the native chemical ligation technique [S1], used for testing Pth hydrolytic activity in cell lysates. Six N-terminal amino acid residues correspond to the sequence of the ErmDL peptide [S2]. Bottom, gel electrophoretic analysis of the products of ErmDL-tRNA hydrolysis after incubation in lysates prepared from wild-type *B. subtilis* cells or from dCas9-containing *B. subtilis* cells with normal (no xylose) or low (with xylose) Pth expression (as described in main Figure 2). Free and peptide-bound tRNA was visualized by ethidium bromide staining.

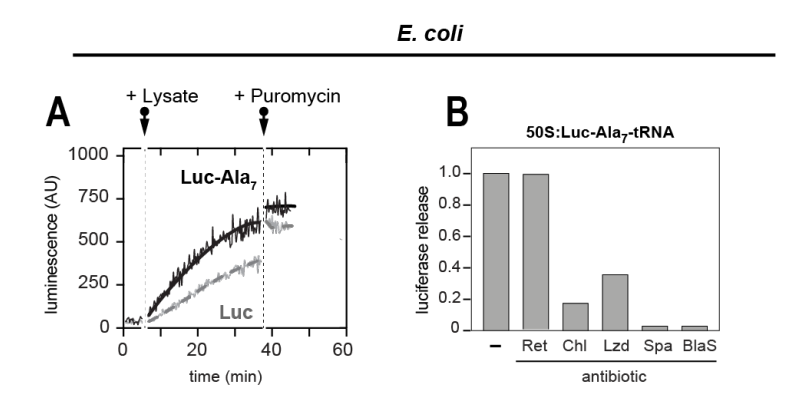


Figure S2. Release of the untailed and Ala₇-tailed Luc from 50S-NCC in *E. coli* lysates (Related to Figure 3A and C). (A) *E. coli* 50S-NCC carrying pept-tRNA with untailed or Ala₇-tailed nascent luciferase were incubated in extracts prepared from wt *E. coli* cells. Complete release of the nascent protein was achieved by subsequent addition of puromycin. Shown is a representative plot of three independent experiments. (B) Effect of ribosome-targeting antibiotics retapamulin (Ret), chloramphenicol (Chl), linezolid (Lzd), sparsomycin (Spa) and blasticidine S (BlaS) upon release of Luc-Ala₇ nascent chain from *E. coli* 50S-NCC by purified *E. coli* Pth. The luminescence values were normalized relative to the no drug control (-).

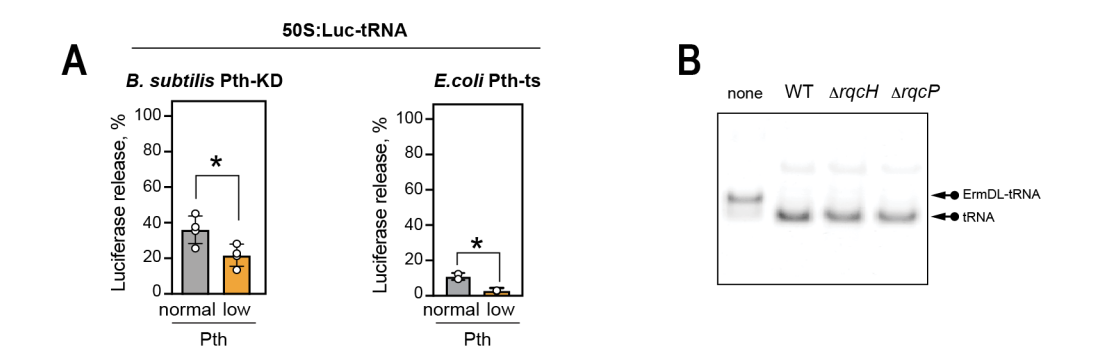


Figure S3. Release of untailed luciferase from 50S subunits in *B. subtilis* or *E. coli* lysates (Related to Figures 2 and 3). (A) Release of untailed luciferase from 50S-NCC in lysates of Pth-KD *B. subtilis* or *E. coli* Pth-ts strains prepared before (normal Pth) and after (low Pth) Pth depletion. The bar graphs represent the efficiency of luciferase release after the 90 min incubation in the lysates estimated relative to the release after subsequent addition of puromycin. The error bars show SD in four independent experiments. (B) Gel electrophoresis showing hydrolysis of free ErmDL-tRNA in lysates from *B. subtilis* wild type, $\Delta rqcH$ or $\Delta rqcP$ cells.

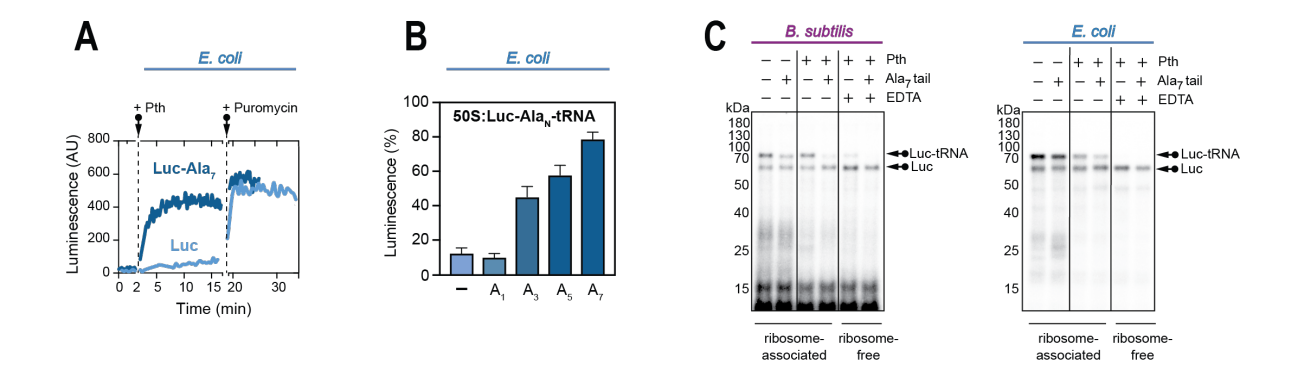


Figure S4. Pth-mediated hydrolysis of ribosome-free and 50S-bound luciferase peptidyl-tRNAs (Related to Figure 4). (A) The release of untailed and Ala₇-tailed luciferase from *E. coli* 50S-NCC by purified *E. coli* Pth. Following 15 min incubation with Pth, complexes were treated with puromycin. (B) Bar graph representing the release efficiencies of nascent luciferase, untailed (-) or C-terminally tailed with the indicated number of alanine residues. Release after puromycin treatment was set as 100%. Error bars show SD in three independent experiments. (C) SDS-gel electrophoresis analysis of pept-tRNA hydrolysis products produced by incubation of *B. subtilis* or *E. coli* 50S-NCC carrying [³⁵S]-labeled LuctRNA or Luc-A₇-tRNA with Pth isolated from the corresponding bacterial species. Addition of EDTA at the beginning of the reaction disassembles 50S-NCC resulting in exposure of free pept-tRNA to Pth. Products were visualized by autoradiography.

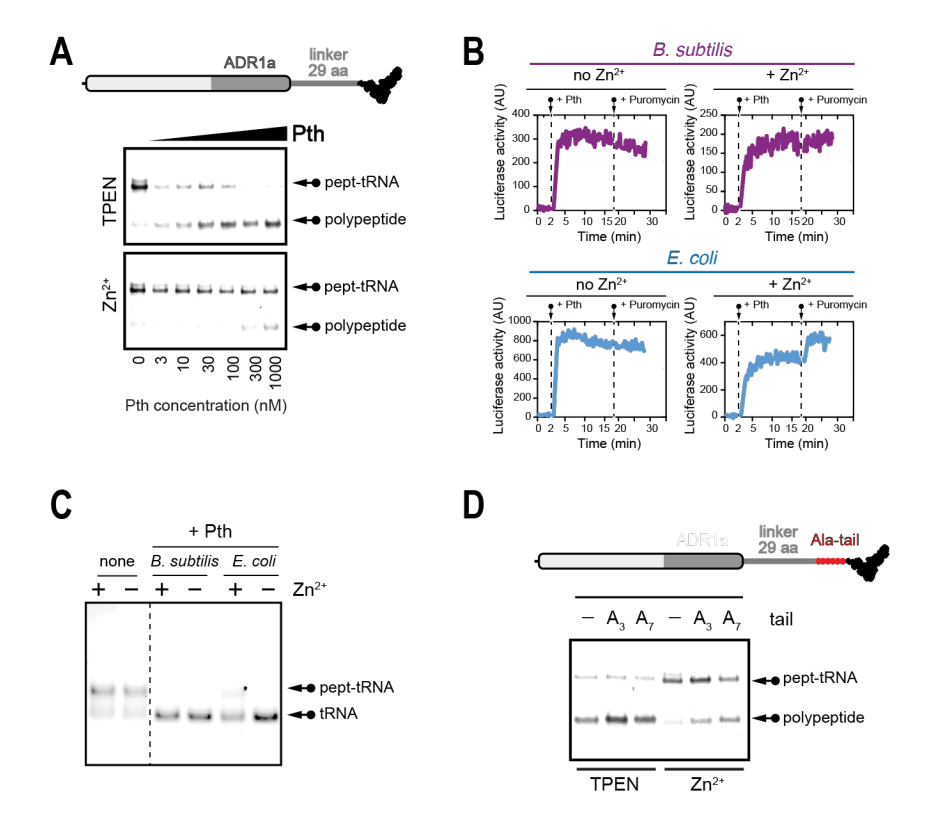


Figure S5. Pth-mediated hydrolysis of ADR1a-containing peptidyl-tRNA stalled in 50S subunits (Related to Figure 5). (A) Hydrolysis products following incubation of *E. coli* 50S-NCC carrying pept-tRNA, resulting from translation of the construct shown on top, with the indicated concentrations of purified *E. coli* Pth. The incubation was performed in the presence of ZnCl₂ (Zn²⁺) or Zn²⁺ chelator (TPEN). (B) Release of luciferase from *B. subtilis* or *E. coli* 50S-NCC carrying Luc-Ala₇-tRNA and treated with Pth purified from the corresponding species in the absence or presence of ZnCl₂. Following incubation with Pth, puromycin was added to release residual nascent luciferase. (C) Hydrolysis of the model pept-tRNA (ErmDL-tRNA) by purified *B. subtilis* or *E. coli* Pth, in the absence or presence of ZnCl₂. (D) Hydrolysis by *E. coli* Pth of pept-tRNA in *E. coli* 50S-NCC where the ADR1a linker (29 aa) was C-terminally extended with none, three or seven alanine residues. In the gels shown in panels B, D, and E, [35S]-labeled peptide product and unreactive peptidyl-tRNA were visualized by autoradiography.

SUPPLEMENTAL INFORMATION REFERENCES

- S1. Syroegin, E.A., Flemmich, L., Klepacki, D., Vazquez-Laslop, N., Micura, R., and Polikanov, Y.S. (2022). Structural basis for the context-specific action of the classic peptidyl transferase inhibitor chloramphenicol. Nat Struct Mol Biol *29*, 152-161.
- S2. Sothiselvam, S., Liu, B., Han, W., Ramu, H., Klepacki, D., Atkinson, G.C., Brauer, A., Remm, M., Tenson, T., Schulten, K., et al. (2014). Macrolide antibiotics allosterically predispose the ribosome for translation arrest. Proc Natl Acad Sci USA *111*, 9804-9809.